Restrictions on Rotational and Translational Diffusion of Pigment in the Membranes of a Rhabdomeric Photoreceptor

TIMOTHY H. GOLDSMITH and RÜDIGER WEHNER

From the Department of Biology, Yale University, New Haven, Connecticut 06520, the Department of Zoology, University of Zurich, Switzerland, and the Marine Biological Laboratory, Woods Hole, Massachusetts 02543

ABSTRACT Individual, isolated rhabdoms from dark-adapted crayfish (*Orconectes, Procambarus*) were studied with a laterally incident microbeam that could be placed in single stacks of microvilli. Concentration gradients of metarhodopsin along the lengths of microvilli were produced by local bleaches, accomplished by irradiation with small spots of orange light at pH 9 in the presence of glutaraldehyde or formaldehyde. No subsequent redistribution of pigment was observed in the dark, indicating an absence of translational diffusion. On the basis of comparison with other systems, glutaraldehyde, but not formaldehyde (0.75%), would be expected to prevent diffusion of protein in the membrane. Under the same conditions photodichroism is observed, indicating an absence of free Brownian rotation. Photodichroism is larger in glutaraldehyde than in formaldehyde, suggesting that the bifunctional reagent quiets some molecular motion that is present after treatment with formaldehyde. Quantitative comparison of photodichroism with mathematical models indicates that the pigment absorption vectors are aligned within ±50° of the microvillar axes and are tilted into the surface of the membrane at an average value of about 20°. The photoconversion of rhodopsin to metarhodopsin is accompanied by an increase in molar extinction of about 20% at the λ_{max} and a reorientation of the absorption vector by several degrees. The transition moment either tilts further into the membrane or loses some of its axial orientation, or both. The change in orientation is 3.5 times larger in formaldehyde than in glutaraldehyde.

INTRODUCTION

The disk membranes of amphibian rod outer segments have recently been shown to be fluid mosaics, consistent with a general model of biological membranes as summarized by Singer and Nicolson (1972). Within the planes of the photoreceptor membranes, the rhodopsin molecules undergo rotational diffusion, with a relaxation time of 20 μs (Cone, 1972). Translational diffusion of visual pigment in the planes of the disks can also be measured across the width of the outer segments (Liebman and Entine, 1974; Poo and Cone, 1974). The measured half-times for diffusional equilibrium are 23–35 s, corresponding to diffusion coefficients 2–6 × 10^{-9} cm^2 s^{-1}.

The bifunctional reagent glutaraldehyde has proved useful in altering the mobility of rhodopsin in amphibian photoreceptor membranes: both translation (Liebman and Entine, 1974; Poo and Cone, 1974) and rotation (Brown, 1972; Cone, 1972) are blocked by the presence of a few percent glutaraldehyde. Treatment with formaldehyde, on the other hand, neither prevents rotation nor slows the rate of translational diffusion (*loc. cit.*). Moreover, in the retinas of an invertebrate (squid) that have been treated with glutaraldehyde, the presence of rhodopsin and its photoproducts, alkaline and acid metarhodopsin, can be demonstrated by means of their fast photovoltages (early receptor potentials) (Hagins and McGaughy, 1967). Glutaraldehyde therefore appears to block diffusional movements of rhodopsin by cross-linking and (at least to a first approximation), neither diffusional movements nor certain other properties of the rhodopsin molecule (spectrum, changes attendant on isomerization) are grossly altered by the presence per se of reactive aldehyde groups.

Although the photoreceptor membranes of arthropods have not been examined as carefully, there are reasons to suspect that they may differ in fluidity. The evidence is based on measurements of dichroic absorption and of the sensitivity of the animals to polarized light. As measurements of dichroism are also a central part of the present work, it is desirable to build on an understanding that begins with the absorption properties of vertebrate outer segments.

The absorption vectors of vertebrate rhodopsin molecules lie roughly coplanar with the disk membranes. As shown in Fig. 1 A, (which follows the terminology of Laughlin et al., 1975, and of Snyder and Laughlin, 1975), absorbance can be resolved into three mutually perpendicular vectors: α_l and α_w in the plane of the membrane and α_h at right angles to the membrane. Because the molecules are free to rotate around axes parallel to α_h, all values of ϕ occur, and $\alpha_l = \alpha_w$. If the molecules were strictly coplanar with the membrane, α_h would be 0. Because the absorption vectors are tilted into the membrane at an angle θ, however, there is some absorption when the e-vector is at right angles to the membrane. Consequently, a stack of such disks viewed from the side (Fig. 1 B) exhibits intrinsic linear dichroism. The absorbance measured with e-vector parallel to the membranes and perpendicular to the axis of the stack $D_\perp$ is several times greater than the absorbance measured with e-vector parallel to the stack. The ratio $R = D_\perp/D_\parallel = \alpha_w/\alpha_h$ has generally been measured to be 3–5 (Liebman, 1962; Wald et al., 1963; Hárosi and MacNichol, 1974*a*, *b*; Hárosi, 1975).

Laughlin et al. (1975) and Israelachvili et al. (1976) have pointed out that measured dichroism in both vertebrate and invertebrate membrane systems will be influenced by the fact that the refractive index is greater for light polarized in the plane of the membrane than at right angles. This form dichroism is given by n_m^4/n_c^4, where n_m and n_c are the refractive indices of the membrane and cytoplasm, respectively. The effect of form dichroism is to underestimate intrinsic dichroism.

One aim of measuring dichroic ratios in photoreceptor cells is to infer the molecular orientations of the pigment molecules. Liebman (1962) has attempted to calculate the tilt angle that the chromophores assume in disk membranes and has derived expressions based on two models: I, all molecules are tilted at some fixed angle which we shall call θ_f; and II, the molecules are randomly distributed

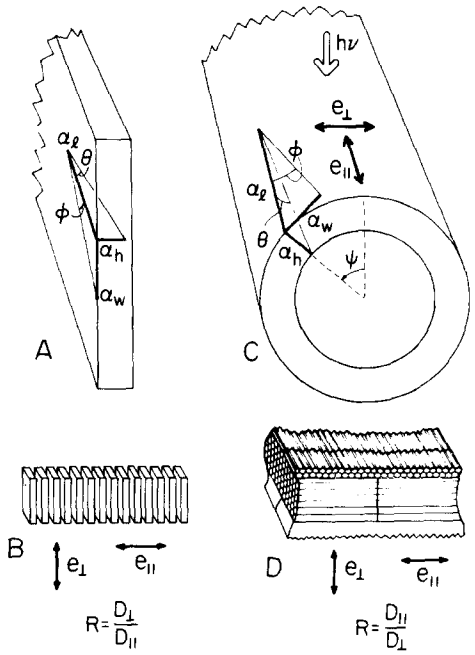

FIGURE 1. Comparison of the photoreceptor membranes of vertebrate outer segments (A, B) and arthropod microvilli (C, D), modified from Laughlin et al. (1975), and Snyder and Laughlin (1975). A, Vertebrate disk membrane. The absorption of a pigment molecule or the population of pigment molecules can be resolved into three orthogonal coefficients, α_l and α_w in the plane of the membrane, and α_h in the "height" or thickness of the membrane. If the transition moment is linear, α_h is produced by its tilt (θ) into the membrane. As the molecules are free to rotate around axes normal to the membrane, all angles ϕ occur. B, The rod or cone outer segment consists of a stack of membranes which exhibit dichroism when viewed from the side. Absorbance with $e_\perp$ is greater than with $e_{||}$ (axes referred to the stack), and the dichroic ratio, $R = D_\perp/D_{||}$. C, The photoreceptor membranes of crayfish are microvilli, but the local absorption coefficients can be defined in an analogous way. θ represents tilt into the membrane; ϕ is measured in the tangent plane of the cylinder, from the microvillar axis. D, The microvilli of crayfish are assembled in bands or layers about 25 μm diam (in the middle of the rhabdom) and 5 μm thick. All the microvilli in one layer are parallel to each other and at right angles to the microvilli of adjacent layers. This diagram shows one complete band and parts of the two contiguous layers. Isolated organelles can be viewed from the side and a small measuring beam placed in a single layer. When the rhabdom's margin appears symmetrically scalloped, "waists" correspond to layers in which the microvilli are viewed from the side, and "hips" to layers in which the microvilli are viewed end-on. The plane of polarization of the measuring beam is referred to the microvillar axes in waists, as shown. In vivo the rhabdom is surrounded by seven retinular cells, but these detach when the tissue is disrupted. In each band there is a central plane, normal to the microvillar axes, which is defined by the closed ends of the microvilli originating from cells on opposite sides of the ommatidium.

through a range of θ, whose limit we shall refer to as θ_d. The calculated values of θ_f and θ_d clearly depend on the measured values of dichroic ratio that one accepts and on whether one adjusts for form dichroism.

The membranes of rhabdomeric photoreceptors are not plane sheets but are rolled into cylindrical microvilli (Fig. 1 C). By analogy, absorbance at any point on the membrane can be resolved into three mutually perpendicular vectors: α_l, parallel to the long axis of the microvillus; α_w, at right angles to α_l but also in a tangent plane; and α_h, in the "height" or thickness of the membrane. The microvilli are arranged in parallel arrays, and in crustacea these form two orthogonal sets (Fig. 1 D). In the eye, light irradiates the microvilli from the side, and it is possible to study individual stacks of parallel microvilli by irradiating small regions of isolated crustacean rhabdoms from the side. It is therefore more convenient to refer the planes of polarization of the measuring beams to the microvillar axes, as defined in Fig. 1 C, D, rather than to the axis of the rhabdom.

Moody and Parriss (1961) were the first to explore theoretically the absorption in such a system, showing that for a random array of chromophores in the tangent planes of the microvilli ($\alpha_h = 0, \theta = 0$, all values of ϕ equally probable, $\alpha_l = \alpha_w$), the dichroic ratio should be 2.0. Any higher dichroic ratio would imply that there is some net orientation of the chromophores with the microvillar axes or, to express the restriction in terms of Fig. 1 C, not all values of ϕ are occupied with equal probability, and the mean value is less than 45°. In the general case ($\theta \neq 0$), the intrinsic dichroism is $2\ \alpha_l/(\alpha_h + \alpha_w)$ and the net dichroism is $2\ R_f\alpha_l/(\alpha_h + R_f\alpha_w)$, where R_f is the form dichroism (Laughlin et al., 1975; Snyder and Laughlin, 1975).

The first measurements of dichroism in crustacean rhabdoms gave values of about 2 which were interpreted as being consistent with the Moody-Parriss (1961) model (Waterman et al., 1969). More recent measurements, however, have yielded higher values with a significant number of examples greater than 3 (Goldsmith, 1975). These results indicate that the chromophores are not randomly oriented in the membrane surface, having some tendency to orientation along the microvillar axes. This conclusion can also be reached by another route. Electrophysiological measurements of the polarization sensitivity of single photoreceptor cells of crustacea (Shaw, 1969; Waterman and Fernandez, 1970; Muller, 1973; Mote, 1974) have yielded values as high as 10–14, and the most likely explanation is that polarization sensitivity is a reflection of dichroic ratio (see discussion of alternatives in Goldsmith, 1975).

Net orientation of chromophores with respect to the microvillar axes implies that Brownian rotation is restricted. If rotational diffusion is not free, this raises the additional possibility that translational movements of the pigment might also be constrained. The purpose of the present work was to test these two hypotheses experimentally, and the results indicate that in crayfish rhabdoms both kinds of movement are indeed restricted. Because the experiments on translational diffusion are conceptually simpler, they are described first. The evidence on rotational diffusion comes from measurements of photoinduced dichroism. In order to analyze these experiments quantitatively, however, it was necessary to develop further the theoretical model in which absorbance in microvilli is

related to molecular orientation. The details are described in the Appendix, with the broad outlines presented in Results. Finally, we have found that the process of isomerization of rhodopsin to metarhodopsin is accompanied by a change in orientation of the transition moment that is equivalent to an increase of several degrees in θ and/or ϕ. A preliminary account of some of this work has appeared in abstract (Goldsmith and Wehner, 1975; Wehner and Goldsmith, 1975).

MATERIALS AND METHODS

Crayfish, usually *Orconectes* (Connecticut Valley Biological Supply, Northampton, Mass.), occasionally *Procambarus* (Carolina Biological Supply, Burlington, North Carolina) were used in this study, generally within 10 days of receipt from the suppliers. Animals were dark-adapted for at least several hours and usually overnight before use. A suspension of tissue fragments including intact rhabdoms from which the surrounding retinular cells had separated was prepared by macerating the eye and eyestalk in 1 ml of van Harreveld's (1936) saline at 0°C in a heavy-walled centrifuge tube, with a stout glass rod. Formaldehyde (prepared from paraformaldehyde to avoid the presence of alcohol) was added to a final concentration of 0.75% (0.25 M), or glutaraldehyde to 2.5%, and the preparation was kept at 0°C for at least 15 min before portions were sampled for study at room temperature. The aldehyde solutions were buffered at about pH 7.2 with *N*-2-hydroxyethylpiperazine-*N'*-2-ethane sulfonic acid (HEPES).

To examine individual rhabdoms, a drop or two of tissue suspension was placed between microscope cover slips and sealed within a ring of silicone vacuum grease. When rapid bleaching of metarhodopsin was desired the sample was made alkaline with a few microliters of a saturated solution of sodium borate. Spectra were recorded with a dual beam recording microspectrophotometer based on the design of Liebman and Entine (1964). Further details of the instrument and data handling can be found in Goldman et al. (1975).

Individual rhabdoms were located with the deep red light of the microscope illuminator filtered with a 712-nm interference filter. As described previously (Waterman et al., 1969; Goldsmith, 1975), it is possible to select rhabdoms and place a microbeam within an individual stack of microvilli, with the direction of propagation of the light either parallel or perpendicular to the microvillar axes (see also Fig. 1).

RESULTS

A. Bleaching of the Pigment

Rhabdoms from dark-adapted eyes show a broad absorption band with λ_{max} near 530 nm at neutral or alkaline pH (Goldsmith, 1977). On brief exposure to light, the absorbance increases and shifts to shorter wavelengths, indicating the formation of a metarhodopsin with λ_{max} near 515 nm. This metarhodopsin is typical of many invertebrates in that it is quite stable in the dark, and the rhabdom undergoes only slow further bleaching (Goldsmith, 1972, 1977). The metarhodopsin can be caused to photobleach, however, in the presence of either glutaraldehyde or formaldehyde and at alkaline pH (Fig. 2). (A possible explanation [Goldsmith, 1977] is that light absorbed by metarhodopsin has a finite probability of converting the chromophore from the all-*trans* not only to ll-*cis*, but to one or more other *cis* isomers as well, and that this creates new conformers of the protein with additional amino groups exposed. At high pH these exist in the

unprotonated form and consequently they react readily with aldehydes. Therefore, the combination of light, free aldehyde, and alkaline pH causes crayfish metarhodopsin to bleach, as illustrated in Fig. 2.) This is a photolysis which

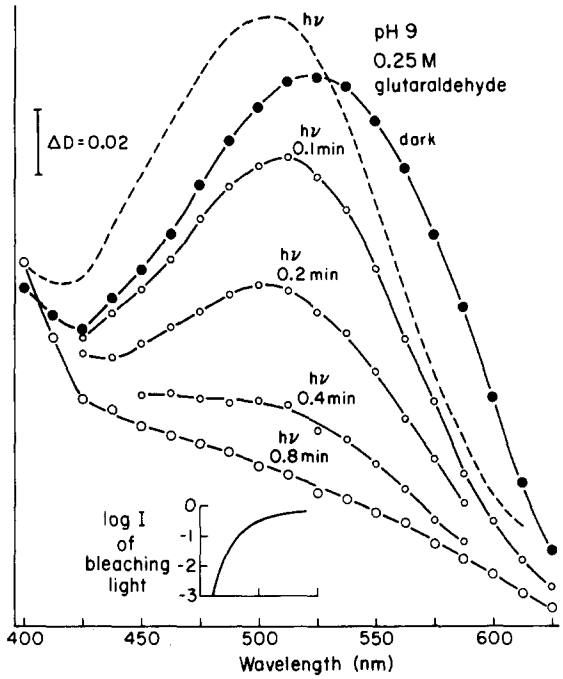

FIGURE 2. Photobleaching of a rhabdom at pH 9 in the presence of 2.5% glutaraldehyde: half-strength van Harreveld's solution. The initial spectrum (*dark*) is shown by the large filled circles. Successive exposures of 0.1, 0.2, 0.4, and 0.8 min to bright yellow light from the field illuminator (Wratten filter no. 9; log transmittance shown in *inset*, whose abscissa runs from 475 to 525 nm) caused the spectrum to shift to shorter wavelengths and fall as shown by the small filled circles. The 0.8 min exposure completed the bleaching, for a second 0.8 min of irradiation caused no additional change. The slope of the final bleached base line is caused principally by light scattering. The 0.1-min irradiation not only caused isomerization of the chromophore and the formation of metarhodopsin, but bleached about one-third of the metarhodopsin as well. The broken curve shows the approximate spectrum immediately after conversion of all the rhodopsin to metarhodopsin, but before any significant photolysis of the latter. This curve cannot be measured under the conditions of this experiment and has been calculated from the difference spectrum of Fig. 12 (e_{II}, little free aldehyde, pH ~7) and a relative molar extinction coefficient of about 1.1, taken from Table I. It shows what existed transiently under these conditions. Spectra were recorded at 22°C and a scanning rate of 20 nm s^{-1}. The measuring beam was polarized parallel to the microvillar axes. Vertical scale is given by the calibration bar in units of absorbance (optical density).

depends on the aldehyde, and is thus different from the formation of alkaline metarhodopsin in cephalopod mollusks (Hubbard and St. George, 1958). Compared to the isomerization of rhodopsin to metarhodopsin, it is slow. A similar

behavior of metarhodopsin in the crustaceans *Libinia* (Hays and Goldsmith, 1969) and *Homarus* (Bruno et al., 1977) has been reported in more detail.

This manner of photobleaching metarhodopsin permits us to examine rhabdoms for the presence of translational diffusion of metarhodopsin by creating local concentration gradients of pigment and looking for a subsequent redistribution of the remaining absorption, as described in section B. Because the rhodopsin and metarhodopsin molecules presumably differ to a small degree in shape but not in weight, one would expect that their diffusion coefficients would be similar. The aldehydes play two roles. They prevent gross structural alterations of the microvilli that are potentiated by light (Waterman et al., 1969; see also Loew, 1976) and that preclude a quantitative analysis of absorbance changes. Second, by hastening the bleaching of metarhodopsin the sensitivity of the system is greatly improved, for the absorbance changes are much larger than those that accompany isomerization at neutral or acid pH. Finally, as described in section D, the same system can also be used to investigate photoinduced dichroism and Brownian rotation.

B. Restrictions on Translational Diffusion

To test for translational diffusion of metarhodopsin, the geometrical arrangement of microvilli was exploited in the following manner. In layers of microvilli in which the long axes of the microvilli were oriented at right angles to the optical axis of the microscope, the plane of abutment of the closed ends of the microvilli arising from opposite sides of the rhabdom marks a plane of membrane discontinuity across which no pigment should be able to diffuse. If a bleaching beam is placed in such a layer and confined to one side of this plane (Fig. 3, I), any bleaching that occurs on the opposite side of the rhabdom must have been caused by scattered light. Moreover, any pigment bleached by the actinic spot cannot be replaced by diffusion from the opposite side of the rhabdom.

When the bleaching light is centered over the central plane, it should deplete pigment from the distal ends of both sets of opposed microvilli. If diffusion of pigment occurs on a time scale similar to that observed in vertebrate photoreceptor membranes, measuring beams subsequently placed anywhere in the same layer of microvilli should record equal concentrations of pigment. This configuration of bleaching and test spots is shown by the diagrams in Fig. 3, II).

Spectra were recorded at sites A and B. By use of deep red light, a small rectangular aperture was then placed in the beam of the field illuminator in the plane of the field stop, and a local, fractional bleach of metarhodopsin was effected. The spectra were rerecorded at the measuring sites; the aperture was removed; a full-field, total bleach was performed; and the final base lines were recorded.

The results of these experiments are also tabulated in Fig. 3. With the bleaching beam confined to one-half of a layer of microvilli, an exposure that bleaches 60–75% of the metarhodopsin under the bleaching beam destroys less than half the pigment on the opposite side of the rhabdom. The same result is obtained when the bleaching beam is centered so as to irradiate the closed ends of both sets of microvilli. It is not surprising that there is no apparent diffusion

of metarhodopsin in the presence of the cross-linking reagent, glutaraldehyde; the important finding is that the same result occurs in 0.75% formaldehyde as well. Because of the different kinetics of photodecay of metarhodopsin in glutaraldehyde and formaldehyde, quantitative comparisons of "fraction

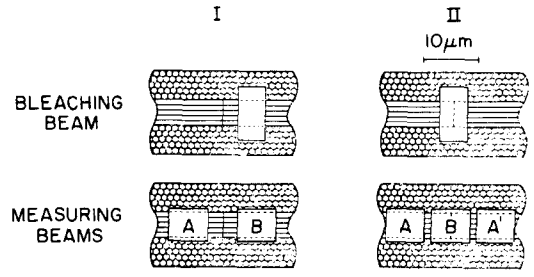

	FRACTION BLEACHED			
	A	B	A(or A')	B
GLUTARALDEHYDE	0.46±0.03 (n=10)	0.76±0.03 (n=10)	0.46±0.04 (n=9)	0.71±0.01 (n=5)
FORMALDEHYDE	0.32±0.03 (n=9)	0.64±0.04 (n=9)	0.37±0.03 (n=22)	0.61±0.02 (n=14)

FIGURE 3. Absence of translational diffusion of metarhodopsin in crayfish rhabdoms. The diagrams at the top, drawn approximately to scale (except for the sizes of the microvilli), show three adjacent layers of microvilli viewed from the side, as well as the placement of bleaching and measuring beams in the central layer. I is a control for light scatter in which the bleaching beam is confined to microvilli on one side of the rhabdom, and pigment is measured at the same site (B) and in the microvilli on the opposite side (A), both before and after the bleaching exposure. II shows the experimental arrangement, in which a centrally placed measuring beam (B) irradiates the terminal 2–3 μm of all microvilli in the layer, and pigment is measured at this site as well as at the opposite ends of the microvilli (A, A'). The bleaching beam was approximately 5 × 10 μm in the object plane, and the measuring beam about 5 × 6 μm. Bleaching exposure was 1 min in 2.5% glutaraldehyde and 1.6 min in 0.75% formaldehyde. Both suspending solutions were approximately 0.5 osM, pH 9 (see Materials and Methods). The bleaching light contained wavelengths longer than 470 nm (Wratten filter no. 9, spectrum in *inset* of Fig. 2) so as to minimize photoregeneration of rhodopsin. A *t*-test of the significance of the difference between the means was performed for the following pairs: glutaraldehyde, I B and II B; formaldehyde, I A and II A; and formaldehyde, I B and II B. None of the differences approaches significance (P = 0.27, 0.34 and 0.42).

bleached" between these two media are not meaningful. The important comparisons are between each experiment (II) and its corresponding control (I). In the presence of either aldehyde, bleaching at sites lateral to the central bleaching beam can be quantitatively accounted for by laterally scattered light. Thus over a time scale of about 2 min, translational diffusion of metarhodopsin along the lengths of the microvilli is not detected.

If the diffusion were very much slower than the rate of photolysis, the asymmetric distribution of metarhodopsin produced during a 1.6-min irradia-

tion should slowly dissipate in the dark, at least in the formaldehyde-treated rhabdoms. The concentration of pigment under the central bleaching site should rise and the concentrations at the edges of the rhabdom should fall. This is not observed. The measurement is complicated, however, by the fact that under our experimenal conditions (free formaldehyde present, pH 9), the metarhodopsin slowly denatures in the dark. Experiments were therefore undertaken to see if the rate of absorbance loss in the dark after a local 1.6-min irradiation was slower under the bleaching slit than at the sides of the rhabdom, as would be the case if slow, lateral diffusion were occurring simultaneously with thermal bleaching. In a given rhabdom, decay at peripheral and central measuring spots appeared to follow first-order kinetics, with identical rate constants at the two measuring sites. Half-times varied in different rhabdoms, however, from 9 to 25 min. The results of five experiments are shown in Fig. 4, where the decay time has been normalized to permit pooling of the data. In a sixth experiment the decay at the two measuring sites could not be described by a single rate constant, but absorbance loss was faster, not slower, at the site of previous irradiation, a result opposite to that expected from a diffusional redistribution of the remaining metarhodopsin.

Put together, the results of Figs. 3 and 4 indicate that there is no detectable diffusion of metarhodopsin over distances of about 10 μm during a time span of about 20 min.

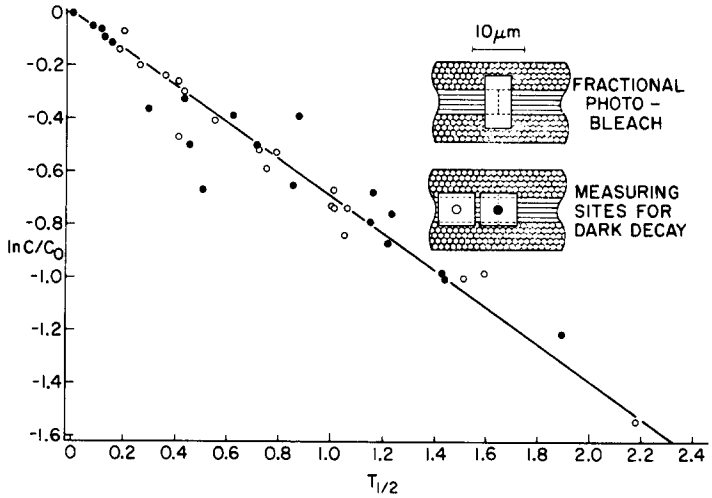

FIGURE 4. First-order dark decay of metarhodopsin that remains after fractional photobleaches. Closed circles: site under the bleaching beam. Open circles: opposite ends of the microvilli. Results are shown for five experiments. In any individual rhabdom, decay at both sites was described by the same rate constant; in order to pool the data from several experiments, however, the time axis has been normalized. $T_{1/2}$ varied in different rhabdoms from 9 to 25 min. Decay of absorbance is described by the same kinetics at sites A and B (terminology of Fig. 3); thus, after a bleaching exposure that destroys part of the pigment, there is no evidence for a slow redistribution of the remaining metarhodopsin along the lengths of the microvilli. Bleaching exposure, 1.6 min, wavelengths longer than 470 nm. Suspending medium included 0.75% formaldehyde, pH 9.

C. Dichroism of Rhabdoms and the Implications for Molecular Orientation

The expression for the dichroic ratio of an array of parallel microvilli,

$$R_0 = \frac{2R_f\alpha_l}{R_f\alpha_w + \alpha_h},$$

(Snyder and Laughlin, 1975), can be modified by replacing the coefficients α_l, α_w, α_h with normalized absorbance coefficients calculated from the angular distributions of chromophores in ϕ and θ (see Figs. 1 and 15, and Appendix). As described in the Appendix, the distribution of axial orientations is assumed to be uniform for all angles smaller than the limiting value, ϕ_d. That is, all angles smaller than the limits of the distribution are allowed and are equally populated. As for molecular tilt into the membrane, we have followed Liebman (1962) and considered two possibilities: model I, all of the absorption vectors are canted into the membrane at a fixed angle θ_f; and model II, the absorption vectors occupy a uniform distribution between $\theta = 0$ and $\theta = \theta_d$.

Eq. (8*a*) and (8*b*) (Appendix) describe the dichroic ratio ($R_0 = D_\parallel/D_\perp$) as a function of ϕ_d and θ_d (or θ_f). The four curves labeled R_0 in Fig. 5 A and B, calculated from Eq. (8*b*), show dichroic ratio as a function of ϕ_d for various assumed values of θ_d and form dichroism. (The curves labeled $R_\parallel$ and $R_\perp$ have to do with photoinduced dichroism and will be described later.) The curves in Fig. 5 A are for extreme cases and assume no form dichroism. The solid curve shows dichroic ratio when the chromophores are virtually confined to the tangent planes of the microvilli ($\theta_d = 0.01°$). The filled circle on the righthand end of the curve corresponds to a random distribution of the chromophores within this plane ($\phi_d = \pm 90°$, all angles therefore occupied), the case originally developed by Moody and Parriss (1961). If the chromophores are more nearly aligned with the microvillar axes (smaller values of ϕ_d), the dichroic ratio rises. The most recent measurements of microvillar dichroism indicate ratios greater than 2.0 (Goldsmith, 1975), implying that not all axial orientations (ϕ) occur with equal probability.

The broken curve (R_0) in Fig. 5 A, on the other hand, shows dichroism when all angles of tilt occur ($\theta_d = 90°$). With this assumption, the maximum dichroic ratio observed is 4.0, even with complete alignment of the chromophores with the microvillar axes ($\phi_d = 0°$). Because measured dichroic ratios of rhabdoms occasionally, and polarization sensitivities of retinular cells frequently, exceed this value (reference above), we also conclude that not all angles of tilt into the membrane are equally probable.

In Fig. 5 B are theoretical plots of dichroic ratio (R_0) calculated on the premise that form dichroism is 1.56 (see below), and for two intermediate values of θ_d, 20° (broken curve) and 40° (solid curve). (As described in the Appendix, 40° is the approximate limit of the distribution of θ_d if the chromophores are tilted into microvillar and rod disk membrane to the same extent [model II].) The open circle on the righthand end of the solid curve R_0 is therefore the expected dichroic ratio in microvilli constructed of membrane with about the same properties as rod disk membrane, merely rolled into cylinders. With random orientation of chromophores ($\phi_d = 90°$), the dichroic ratio is 1.67 rather than 2.0

(Snyder and Laughlin, 1975). Higher dichroic ratios can be achieved by decreasing either θ_d or ϕ_d, or both.

Compared to the orientation parameters, the value of form dichroism has a relatively small influence on the dichroic ratio. Fig. 6 shows dichroic ratio (R_0) as

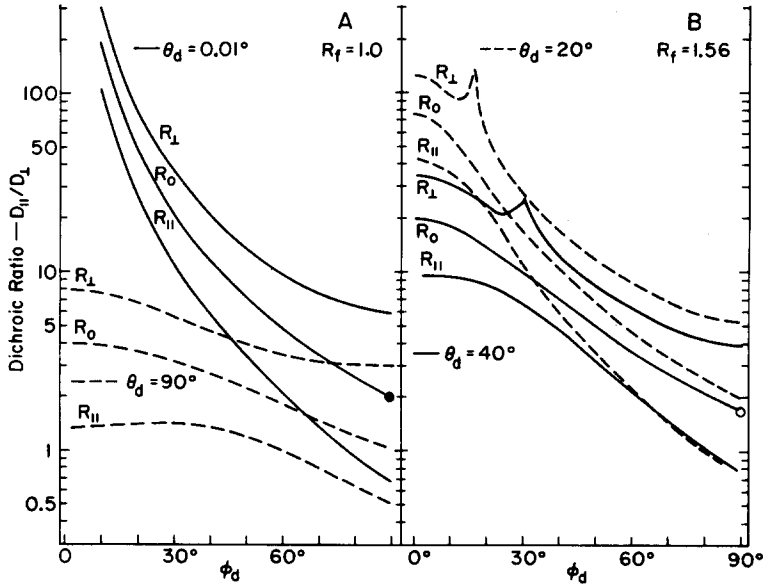

FIGURE 5. Theoretical plots of microvillar dichroism as a function of the limit of the distribution of axial orientation, ϕ_d, for various assumed values of θ_d (limit of the distribution of chromophore tilt) and R_f (form dichroism). Dichroic ratio ($R = D_{\parallel}/D_{\perp}$) is defined as [absorbance measured with e-vector parallel to the microvilli]/[absorbance with e-vector perpendicular to the microvilli]. R_0, the dichroic ratio of dark-adapted microvilli, is calculated from Eq. (8*b*). $R_{\parallel}$, dichroism after a fractional bleach with the e-vector of the actinic beam polarized parallel ($e_{\parallel}$) to the microvilli, as calculated from Eq. (11*b*, with $k_{\parallel} = k_{\parallel max}$, as defined in the Appendix. Similarly, $R_{\perp}$, the dichroic ratio after a fractional bleach with $e_{\perp}$, is calculated from Eq. 14*b*, with $k_{\perp}$ at its maximum value. Fig. 5 A shows results for two extreme cases: the chromophores confined to the tangent planes of the microvilli ($\theta_d \simeq 0°$), and all angles of tilt allowed ($\theta_d = 90°$). Form dichroism is assumed to be absent. The lower terminus of the solid curve labeled R_0 (filled circle) is the condition described in the model of Moody and Parriss (1961), (random orientation of chromophores in the tangent planes of the microvilli) and corresponds to a dichroic ratio of 2.0. Fig. 5*B* shows results of calculations for two intermediate values of θ_d and with form dichroism of 1.56. See text for further details.

a function of form dichroism (R_f) for one specific solution of Eq. (8*a*) (model I) and two specific solutions of Eq. (8*b*) (model II). The values of ϕ_d, θ_d, and θ_f used in these calculations were selected on the basis of experimental results described in a section that follows; however, the important point to note at this juncture is that a maximum uncertainty in R_f leads to an error in R_0 of only ±10%. In what follows, therefore, we need to sustain only a modest interest in

the value of form dichroism selected for calculation, a convenient circumstance as R_f has not yet been reliably measured. A study of the birefringence of isolated crayfish rhabdoms has yielded estimates of form dichroism of 1.26 and 1.56 under different experimental conditions (Goldsmith and Paulson, Unpublished observations).

D. Photoinduced Dichroism

If individual metarhodopsin molecules are not able to rotate through all angles limited by $\pm\phi_d$ in the tangent planes of the microvilli, it should be possible to

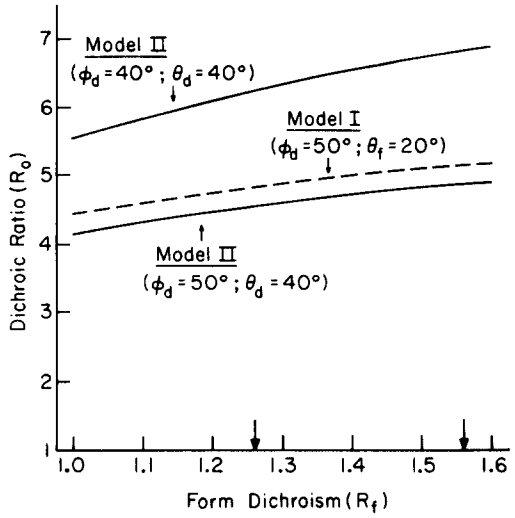

FIGURE 6. Shallow dependence of dichroic ratio (R_0) on form dichroism (R_f), calculated from Eq. (8*a*), model I, and from Eq. (8*b*), model II. (The specific values of ϕ_d, θ_d, and θ_f that have been used in the calculation are drawn from analyses of photodichroism, as described later). See text.

increase the dichroic ratio by bleaching part of the population with light polarized perpendicular to the microvilli ($e_\perp$) and to decrease the dichroic ratio with a bleaching light having parallel e-vector ($e_\parallel$). After such a fractional bleach, the remaining pigment should therefore exhibit photoinduced dichroism. As with vertebrate photoreceptor membranes, photoinduced dichroism in the presence of the cross-linking reagent glutaraldehyde would not be surprising, but photoinduced dichroism in the presence of formaldehyde would be evidence that Brownian rotation does not occur freely. Figs. 7 and 8 show two examples of rhabdoms treated with formaldehyde in which photodichroism has been induced. In the experiment of Fig. 7 the dichroic ratio was increased from 2.46 to 3.39 by a fractional bleach with $e_\perp$. In Fig. 8 the dichroic ratio was decreased from 2.37 to 1.83 by a partial bleach with $e_\parallel$.

The initial spectra in Figs. 7 and 8 reflect the presence of rhodopsin. After a partial bleach with orange light, however, only metarhodopsin remains. In order to minimize changes in absorbance due to the conversion of rhodopsin to

metarhodopsin, measurements were made at the isosbestic wavelengths. The essential point of Figs. 7 and 8 is not the precise value of dichroic ratio, but that dichroic ratio of the metarhodopsin can be either increased or decreased, depending on the plane of polarization of the bleaching light.

Experiments such as those in Figs. 7 and 8 indicate that the metarhodopsin molecules cannot turn through all values of ϕ. In order quantitatively to analyze

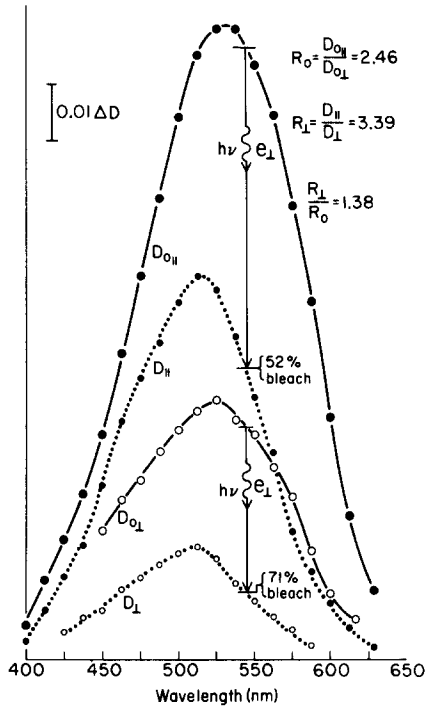

FIGURE 7. Photodichroism: example of an experiment in which the dichroic ratio of a layer of microvilli was increased from 2.46 to 3.39 by a fractional bleach with light polarized perpendicular ($e_\perp$) to the microvillar axes. (See Fig. 1 for axes of reference.) Spectra were recorded initially, after several seconds' exposure to the polarized actinic beam, and again after a 2-min irradiation with unpolarized light that bleached all remaining pigment. Difference spectra (in units of absorbance) were calculated by subtracting the final bleached base line from each of the earlier spectra: $D_{0\parallel}$, optical density measured with $e_\parallel$ for the full complement of pigment; $D_{0\perp}$, the same, but measuring beam with $e_\perp$; $D_\parallel$, optical density of pigment (now metarhodopsin), measured with $e_\parallel$, remaining after a partial bleach with $e_\perp$; $D_\perp$, the same, but measured with $e_\perp$. R_0, initial dichroic ratio; $R_\perp$, dichroic ratio after partial bleach with $e_\perp$; $R_\perp/R_0$, photodichroism. Fraction bleached is calculated at a wavelength near the isosbestic point for the rhodopsin-metarhodopsin conversion; therefore, changes in absorbance at this wavelength measure the amount of metarhodopsin bleached and are not affected by absorbance changes associated with the conversion of rhodopsin to metarhodopsin. The pH was ~9 and the suspending medium contained 0.75% formaldehyde. The bleaching light was yellow (see *inset*, Fig. 2).

this kind of result, however, it is necessary to develop further the model of microvillar dichroism. This has been done in Appendix B. $R_{\parallel}$, the dichroic ratio after fractional bleaches with $e_{\parallel}$, is given by Eq. (11*a*) (model I) and (11*b*) (model II); $R_{\perp}$, the dichroic ratio after a fractional bleach with $e_{\perp}$, is given by Eq. (14*a*) (model I) and (14*b*) (model II). The only additional assumption made in deriving Eq. (11*a*, *b*) and (14*a*, *b*) is that the probability that a molecule will be bleached is directly proportional to its probability of absorption.

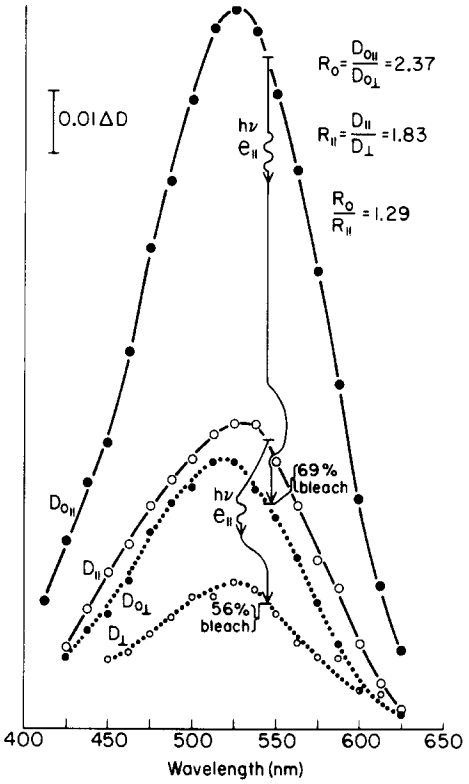

FIGURE 8. Photodichroism: example of an experiment in which the dichroic ratio of a layer of microvilli was decreased from 2.37 to 1.83 by a fractional bleach with light polarized parallel ($e_{\parallel}$) to the microvillar axes. Labeling and other experimental details otherwise as described in the caption to Fig. 7.

Fig. 5 A, B shows the dichroic ratios $R_{\parallel}$ and $R_{\perp}$ for each of the cases of R_0 discussed in section C. In each instance the hypothetical bleach was "saturating," in that $k_{\parallel}$ and $k_{\perp}$ were assigned their maximal values (see Appendix). Examination of the curves in Fig. 5 shows that photoinduced dichroism can be expected to alter the dichroic ratio by a factor of approximately 1.5–3.0 ($R_{\perp}/R_0$ or $R_0/R_{\parallel}$) over a wide range of values of ϕ_d, θ_d, and R_f. (The cusps on the curves for $R_{\perp}$ in Fig. 5 B are of little practical significance; they occur when Eq. (13*c*) and (13*d*) give the same value for $k_{\perp max}$).

Model I generates curves similar to those in Fig. 5, except (*a*) the values of θ_f are about half as large as θ_d for equivalent values of R_0, and (*b*) with θ fixed,

corresponding curves of R_0, $R_\parallel$, and $R_\perp$ converge for low values of ϕ_d. This is because when the population of chromophores occupies a limited distribution of angles, there is less photodichroism. In the limiting case (ϕ and θ both fixed), there is no possibility of photoinducing dichroism with $e_\parallel$, and $R_\parallel = R_0$.

In order to apply the mathematical model to experimental data, two transformations are made; the first is convenient, the second is necessary. Photoinduced dichroism is defined as $R_\perp/R_0$ and $R_0/R_\parallel$, thereby restricting attention to the change in dichroic ratio induced by the bleaching beam, and facilitating comparison between results with $e_\parallel$ and $e_\perp$ bleaching lights. Photoinduced dichroism, thus defined, is a positive number larger than 1.0. Second, photoinduced dichroism must be related to some measurable parameter. Degree of bleach in the optimal angle (i.e. expressed in terms of fractions of $k_{\parallel max}$ and $k_{\perp max}$) cannot be measured directly; however, fractional absorbance loss, measured with light polarized parallel to the e-vector of the bleaching beam, can.

Fig. 9 shows theoretical curves for photoinduced dichroism as a function of the fraction of the pigment—measured with e-vector coincident with the plane of polarization of the bleaching beam—that has been bleached. The curves in Fig. 9 were calculated for $\theta_d = 40°$ and $R_f = 1.26$; but as the value of R_f has a small effect, they therefore correspond to a case very similar to that shown with the solid curves in Fig. 5 B. As Fig. 9 indicates, the model makes two interesting predictions. First, the magnitude of the photoinduced dichroism depends on the

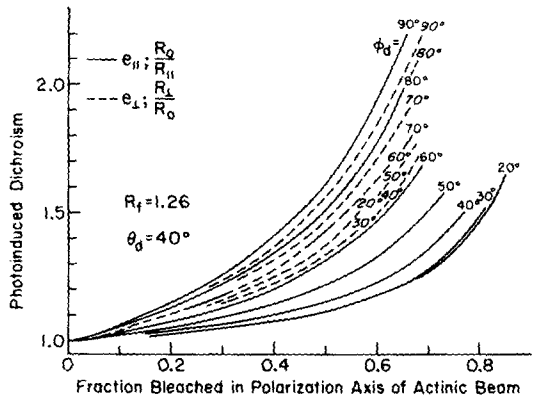

FIGURE 9. Theoretical plots of photoinduced dichroism in microvilli, $R_0/R_\parallel$ or $R_\perp/R_0$, vs. fraction of the absorbance (measured with e-vector parallel to the plane of polarization of the actinic beam) that has been bleached, and based on model II. Fraction bleached = $(D_{0\parallel} - D_\parallel)/D_{0\parallel}$ or $(D_{0\perp} - D_\perp)/D_{0\perp}$, where D_0 is the initial density (absorbance) of pigment, D is the absorbance after a fractional bleach, and the subscripts $\parallel$ and $\perp$ refer to the plane of polarization of the measuring beam with respect to the microvillar axes. Absorbances are based on partial and total bleaches, thereby eliminating the effect of light scatter. R_0 = initial dichroic ratio (from Eq. [8]); $R_\parallel$ = dichroic ratio after a fractional bleach with e-vector parallel ($e_\parallel$) to the microvilli (from Eq. [11 *b*]); $R_\perp$ = dichroic ratio after fractional bleach with $e_\perp$ (from Eq. 14 *b*). Each family of curves shows expected results for various values of ϕ_d on the assumption that $\theta_d = 40°$, and the form dichroism (R_f) is 1.26. Solid curves are for bleaching light with $e_\parallel$; broken curves for a bleaching light with $e_\perp$. For most values of ϕ_d, the curves for $e_\perp$ lie above their counterparts for $e_\parallel$.

degree of orientation of the chromophores with the microvillar axes, being smaller (for any given fraction bleached), the smaller is ϕ_d. Thus a family of curves is required to show all possible degrees of photodichroism as a function of fraction of pigment bleached. Second, for any fraction bleached, and for all but the largest values of ϕ_d, the magnitude of the photoinduced dichroism depends on the plane of polarization of the bleaching beam, being greater for $e_\perp$ than for $e_\parallel$. This is shown by the fact that for $\phi_d < \pm 80°$, curves in the family drawn with dashed lines ($e_\perp$) lie above their counterparts in the family drawn with solid lines ($e_\parallel$).

The theoretical curves in Fig. 9 are based on the assumption that individual molecules have been frozen in place, as might be achieved in glutaraldehyde. In formaldehyde, however, the molecules might continue to wobble within the allowed distribution. It this happened, the photoinduced dichroism would be less than expected for a rigid array. (This can be understood by recalling the limiting case, turning through ±90°, for which where should be no photoinduced dichroism, and all points should plot on the abscissa in graphs of the form of Fig. 9.) Fig. 10 compares experimental results obtained in glutaraldehyde and

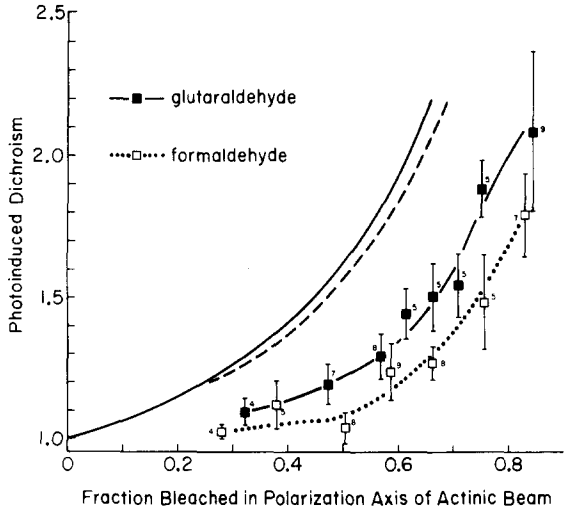

FIGURE 10. Photoinduced dichroism of crayfish rhabdoms fixed in glutaraldehyde (filled circles) and formaldehyde (open circles). The two uppermost curves are theoretical functions indicating the expected photodichroism if all possible axial orientations of chromophore occurred with equal frequency ($\phi_d = 90°$) and the population was "frozen" in place by the treatment with glutaraldehyde. (Solid curve is for $R_0/R_\parallel$; broken curve for $R_\perp/R_0$; $\theta_d = 40°$; $R_f = 1.26$.) The curves through the data points have no theoretical significance. That the experimental points fall well under the two theoretical curves indicates that the absorption vectors have a significant net orientation with respect to the microvillar axes (compare Fig. 9). The numeral by each data point is the number of rhabdoms entering the average. Vertical error bars indicate ±1 SE, and the data have been grouped so that the horizontal error bars are all smaller than the symbols marking the data points. An analysis of variance indicates that the photodichroism in glutaraldehyde is significantly greater than in formaldehyde ($P < 0.01$).

formaldehyde. As anticipated, both curves lie well under the theoretical functions for $\theta_d = \pm 90°$. The points for rhabdoms in glutaraldehyde, however, fall above those in formaldehyde, suggesting that the bifunctional aldehyde has quieted some molecular motion that is present in formaldehyde.

Fig. 11 is a further analysis of results obtained in the presence of glutaralde-

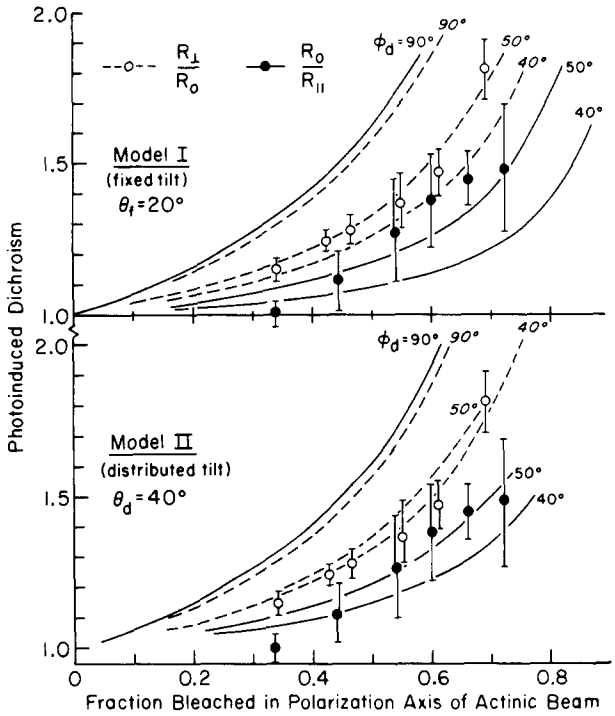

FIGURE 11. Comparison of measurements of photodichroism with theroretical curves. Model I, the chromophores are assumed to be tilted into the membrane at a fixed angle (θ_f) of 20°. Filled circles give photodichroism ($R_0/R_\parallel$) after fractional bleaching with $e_\parallel$; open circles show photodichroism ($R_\perp/R_0$) after bleaching with $e_\perp$. In each case, the photodichroism increases with fraction of pigment bleached and, as predicted by theory, the points for $e_\perp$ lie above those for $e_\parallel$. As shown by the theoretical functions, the data fit reasonably well the curves for $\phi_d = 50°$. Fit deteriorates as θ_f departs as much as 10° from the value shown. Model II, the filled circles follow $\phi_d = 50°$; the open circles appear to fit slightly better the curve for $\phi_d = 40°$. Other values of θ_d (not shown) give less satisfactory fits. Both model I and model II therefore agree in indicating that the chromophores lie within a fan of about ±50° with the microvillar axis.

hyde in which the data for $e_\parallel$ and $e_\perp$ bleaching lights are treated separately. Here, too, there is a difference. Greater values of photodichroism are observed when the bleaching light is polarized perpendicular to the microvilli, as predicted by theory. The upper half of the figure compares the data with the predictions of model I. R_f is assumed to be 1.26 and $\theta_f = 20°$. There is a good fit to $\phi_d = 50°$, which cannot be improved by other choices of θ_f. The lower half of the figure shows the comparison with model II. R_f is 1.26, and $\theta_d = 40°$.

Theoretical curves for $\phi_d = 40°$ and 50° are shown and, as before, the fit is not readily improved by other choices of tilt parameter. If θ_d is made grossly smaller, it becomes more difficult to fit the data for $e_{\parallel}$ and $e_{\perp}$ with curves that have a common value of ϕ_d. The results may therefore be taken as a reasonable estimate of the orientation parameter ϕ_d, indicating that the absorption vectors lie within ±50° of the microvillar axes. The implications for polarization sensitivity will be examined in the Discussion.

E. Change in Orientation on Isomerization

Fig. 12 shows the difference spectrum for the conversion of visual pigment to metarhodopsin when the rhabdoms are suspended in a medium containing 2.5% glutaraldehyde. In order to slow the subsequent destruction of metarhodopsin, the pH was 7.4 rather than 9. Results are shown for measurements with the e-vector of the measuring beam parallel (closed circles) and perpendicular (open circles) to the axes of the microvilli, and the difference spectra have been normalized at the long wave-length peak of the difference spectrum (wavelength of maximum absorbance decrease). The curves for $e_{\parallel}$ and $e_{\perp}$ are not identical, as there is a relatively greater increase in absorbance for $e_{\perp}$. If the dichroic ratio for the initial (dark) pigment were the same as for metarhodopsin, the difference spectra should be superimposible. The relatively greater increase in absorbance with $e_{\perp}$ means that the dichroic ratio of metarhodopsin must be smaller than the dichroism of the pigment originally present.

Fig. 13 shows the same difference spectra when the rhabdoms are in 0.75% formaldehyde. The results are qualitatively similar, but the difference between the curves for $e_{\parallel}$ and $e_{\perp}$ is even greater than in glutaraldehyde. The change in molecular orientation that accompanies isomerization must therefore be larger in formaldehyde than in glutaraldehyde.

In glutaraldehyde, the positive peak in the normalized difference spectrum reaches values of 0.8 for $e_{\parallel}$ and 1.0 for $e_{\perp}$. If there were no changes in orientation of the chromophoric region, the difference spectra should both peak at some intermediate value. Both 0.8 and 1.0 fall below the corresponding values of 1.1 and 2.1 obtained in formaldehyde. In other words, any possible intermediate value for the peak of the difference spectrum in formaldehyde lies outside the range observed in glutaraldehyde. This means that in formaldehyde compared to glutaraldehyde, not only is there a greater orientation change accompanying isomerization, but apparently a relatively greater increase in molar extinction coefficient is involved as well. That is, if $\epsilon^{meta}_{\lambda_{max}}$ is the molar extinction coefficient of metarhodopsin at the λ_{max}, and $\epsilon^{rhod}_{\lambda_{max}}$ the same for rhodopsin, the ratio $\epsilon^{meta}_{\lambda_{max}}/\epsilon^{rhod}_{\lambda_{max}}$ seems to be greater in formaldehyde than in glutaraldehyde.

The method used to disentangle the orientation parameters from the ratios of molar absorbance is described in detail in the Appendix. Its application depends on knowledge of the shapes of the difference spectra for total bleaches and for metarhodopsin in the presence of both glutaraldehyde and formaldehyde. These are available from experiments (Goldsmith, 1977). The analysis also rests on the assumptions that (*a*) a brief irradiation with orange light converts virtually all the rhodopsin to metarhodopsin, and (*b*) metarhodopsin is the only photoproduct. Brief successive exposures to the actinic source indicate that the first

condition is met. Experiments on the photobleaching of metarhodopsin indicate that it is spectrally homogeneous (Goldsmith, 1977) and, as with other arthropods, there is as yet no evidence for the formation of isorhodopsin. As metarhodopsin is bleached, photoproducts are formed with absorption maxima at

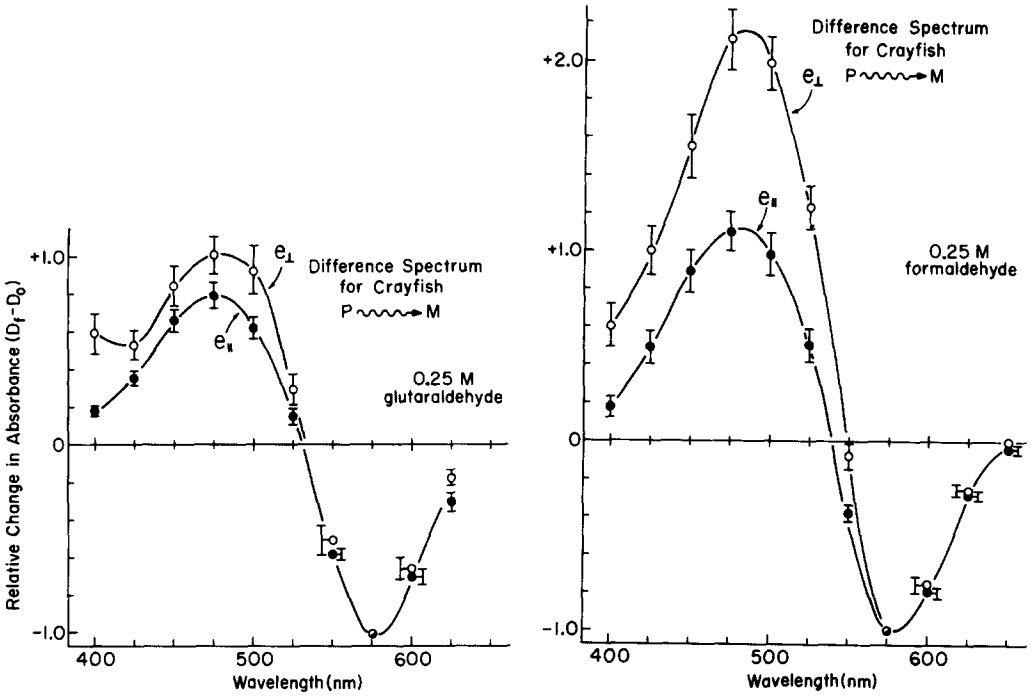

FIGURE 12. (*Left*) Difference spectrum for the photoconversion of the original pigment to metarhodopsin, after fixation in 2.5% glutaraldehyde. In order to minimize bleaching of metarhodopsin, the isomerizing exposure was 0.05 min, the (unpolarized) light contained only wavelengths longer than 585 nm, and the pH was 7.4. These conditions permit complete conversion to metarhodopsin with no measured bleaching of metarhodopsin. Average of 10 experiments (±SEM), normalized at the wavelength of maximum absorbance decrease. Note that the shape of the difference spectrum depends on the plane of polarization of the measuring light.

FIGURE 13. (*Right*) Difference spectra for the photoconversion to metarhodopsin in the presence of 0.75% formaldehyde. Experimental conditions otherwise as described in the caption to Fig. 12. Average of nine experiments normalized at 575 nm, the wavelength of maximum absorbance loss. Note that in formaldehyde the shape of the difference spectrum is more sharply dependent on the plane of polarization of the measuring light than it is in glutaraldehyde (Fig. 12).

shorter wavelengths, but the difference spectra of Figs. 12 and 13 were measured under conditions designed to minimize the destruction of metarhodopsin. Moreover, the analysis is based on absorbance changes at 475 nm and 575 nm, wavelengths where absorption by such final photoproducts is not great. We therefore believe the second assumption is also valid.

Results of calculations are shown in Table I. With model I, in the presence of glutaraldehyde the relative molar extinction ($\epsilon^{meta}_{\lambda_{max}}/\epsilon^{rhod}_{\lambda_{max}}$) is 1.09, and in the presence of formaldehyde it is 1.20. In neither case is the result strongly dependent on the values of form dichroism or the range of orientation parameters assumed. If one assumes that all of the orientation change that accompanies isomerization takes place as an increase in either ϕ_d or θ_d, the change in either case is about 0.9° in glutaraldehyde and 3.1° in formaldehyde.

If model II is applied, the results are similar except that the increase in the fan of tilt angles is about 6°. For both models and each assumed set of conditions, however, the orientation change in formaldehyde is ~3.5 times larger than in glutaraldehyde.

TABLE I

CHANGE IN ORIENTATION AND RELATIVE MOLAR EXTINCTION WITH ISOMERIZATION

	$\phi_d' - \phi_d$*	$\theta_f' - \theta_f$‡ or $\theta_d' - \theta_d$§	$\epsilon^{meta}_{\lambda max}/\epsilon^{rhod}_{\lambda max}$‖
Model I			
Formaldehyde	3.05°±0.14°¶	2.98°±0.80°	1.20±0.01
Glutaraldehyde	0.88°±0.06°	0.84°±0.17°	1.09
Model II			
Formaldehyde	3.26°±0.17°	5.94°±1.16°	1.20±0.01
Glutaraldehyde	0.92°±0.05°	1.66°±0.31°	1.09

* Calculated for $\phi_d' = 40°$ and 50°; $R_f = 1.26$ and 1.56.

‡ $\theta_f' = 20°$.

§ $\theta_d' = 40°$.

‖ $\epsilon^{meta}_{\lambda max}/\epsilon^{rhod}_{\lambda max} = N_{\lambda max}/M_{\lambda max}$; see Discussion for an alternative interpretation of the results in this column.

¶ Median and range of calculated values.

F. Absence of Anisotropic Scatter

The experiments on local bleaching demonstrated the presence of significant lateral scatter of a small bleaching beam. Presumably, the measuring beams, too, are subject to an equivalent scattering by the rhabdom. In interpreting microspectrophotometric measurements made with plane-polarized light, it becomes important to know the extent to which the measuring beam is depolarized by scatter. Fig. 14 shows the form of an experiment designed to answer this question. Bleached rhabdoms were placed on the stage of a polarizing microscope with the optic axes of the birefringent layer either parallel or perpendicular to the transmission axis of the polarizer. A mask was placed in the plane of the field stop so that its image snugly framed the rhabdom, as shown by the diagram in Fig. 14. A photomultiplier tube was coupled to the trinocular head of the microscope, and the intensity of light transmitted by the rhabdom was measured as a function of the angle, ϕ, between polarizer and analyzer. Further details are given in the caption to Fig. 14.

As Fig. 14 shows, the intensity fell to less than 1% of its full value without departing from the $\cos^2\phi$ function, indicating that the scattered light collected by the microscope objective is not significantly depolarized. This in turn demonstrates that depolarization by scatter is not degrading our microspectrophotometric measurements of dichroism.

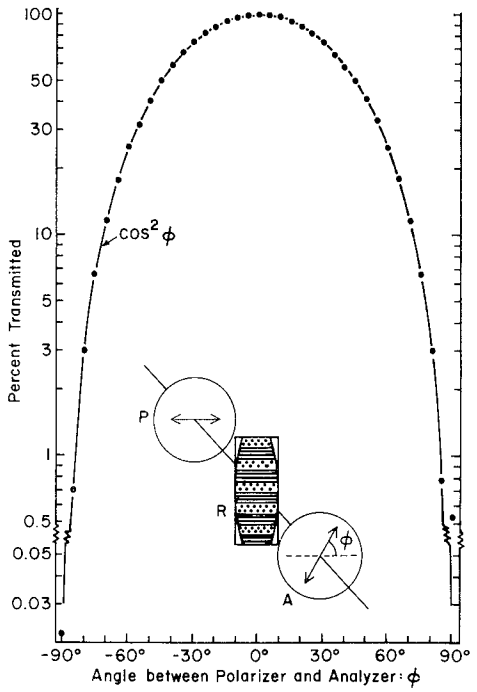

FIGURE 14. Linearly polarized light is not significantly depolarized as a consequence of scatter on passing laterally through a rhabdom. *P*, polarizer; *A*, analyzer; and *R*, rhabdom surrounded by a mask (placed in the plane of the field stop) and oriented with the optic axes of individual layers of microvilli either parallel or perpendicular to the transmission axes of the polarizer to eliminate rotation due to birefringence. Transmitted intensity was measured with a photomultiplier as a function of ϕ, the angle between the polarizer and analyzer. With crossed polarizers, less than 0.7% of the light is transmitted, indicating that virtually all the light passing through the organelle into the collecting optics has maintained its plane of polarization. The wavelength band was broad (440–580 nm), and the numerical aperture of the collecting lens was 0.85, compared with 0.4 on the microspectrophotometer.

DISCUSSION

Use of Aldehyde Fixatives

As the apparent absence of diffusion of metarhodopsin in crayfish photoreceptor membranes is observed after treatment with formaldehyde, it is appropriate to explore the significance of this condition.

Brown (1972) reported that vertebrate photoreceptors fixed for 5–6 h in 5% formaldehyde at 25°C failed to exhibit photodichroism (and thus were still fluid), an observation confirmed by Cone (1972). Edidin et al. (1976) found that 0.5% formaldehyde had no effect on the diffusion of fluorescein-labeled membrane proteins of mouse fibroblasts, but they did observe that in this system 5% formadehyde blocked movement. In our experiments, 0.75% formaldehyde was used, and the rhabdoms were kept at 0°C for varying periods of time (several minutes to several hours) before measurement at 20–22°C. On the basis of this other work with membrane protein it therefore does not seem likely that in our experiments the absence of diffusion of metarhodopsin was caused by the presence of formaldehyde. Although this conclusion needs a more rigorous proof, it is supported by two additional arguments.

First, there clearly are differences between glutaraldehyde- and formaldehyde-fixed rhabdoms in the extent to which the metarhodopsin molecules can move or change shape: (*a*) the greater photodichroism in glutaraldehyde-fixed material (Fig. 10) indicates that this reagent damps out some Brownian chatter that persists in formaldehyde; (*b*) the smaller change in orientation on isomerization in glutaraldehyde (Figs. 12, 13; Table I) bespeaks either a more rigid microenvironment or constraints on the possible conformational changes the molecule can undergo, or both.

A second argument is perhaps more compelling. The presence of photoinduced dichroism requires the absence of molecular rotation. If Brownian rotation were normally present but were artifactually eliminated by aldehyde fixation, both glutaraldehyde and formaldehyde might "freeze" the population of molecules so that all normally allowed angles of axial orientation would be occupied. But the measurements of photodichroism fall well under the theoretical curves for $\phi_d = \pm 90°$, indicating that not all axial orientations occur with equal probability (Figs. 10, 11). In other words, the measurements of photodichroism made in the presence of glutaraldehyde, where we expect cross-linking (Richards and Knowles, 1968) to have blocked molecular diffusion, provide another line of evidence that free Brownian rotation does not occur. It should be recognized, however, that this argument carries the burden of its own assumption, namely, that fixation does not arrest molecular rotations with the transition moments in certain preferred orientations.

Basis for the Absence of Diffusion

The concept of membranes as fluid mosaics is supported by much evidence (Singer and Nicolson, 1972) including diffusional studies on cells other than photoreceptors (Edidin, 1974). The few quantitative estimates of diffusion constant that have been reported, however, suggest that there may be variation in membrane fluidity among different kinds of cells. In lower organisms there is a wide range (several tens of degrees centigrade) of lipid phase transition temperatures, depending on conditions of growth (e.g., Steim et al., 1969; Overath et al., 1970; Eletr and Keith, 1972; Murata et al., 1975). Although the presence of cholesterol in the plasma membranes of higher animals obscures such transitions (Edidin, 1974), differences in fluidity may well occur between species of animal as distantly related as frog and crayfish. Israelachvili and

Wilson (1976) have suggested that the fact that microvilli are neither planar nor spherical—and thus lack constancy of curvature over their surfaces—is in itself evidence that the membranes are rigid. The rhabdoms of squid are reported to exhibit dichroic ratios as high as 6 (Hagins and Liebman, 1963). The photoreceptor membranes of crayfish may therefore be intermediate in fluidity between rod outer segment disks and the purple membrane of *Halobacterium*, with its highly ordered bacteriorhodopsin molecules (Henderson and Unwin, 1975).

Vertebrate photoreceptor membranes are characterized by a very low content of cholesterol and a high content of long-chain polyunsaturated fatty acids (see Daemen, 1973, for review), conditions that may be responsible for the relatively rapid diffusion of rhodopsin in these organelles. Corresponding lipid analysis of rhabdomeric membranes are not as numerous, but data now available indicate that squid (Mason et al., 1973), *Limulus* (Benolken et al., 1975), and insects (Zinkler, 1975) have several times as much cholesterol as, and probably a somewhat lower content of polyunsaturated fatty acids than vertebrate rods. This implies that their membranes may be stiffer and diffusion of rhodopsin correspondingly slower. As no analyses of the lipid content of crayfish rhabdoms have been done, the argument cannot be carried further at this point.

Basis for Molecular Orientation

Although a relatively stiff lipid environment could explain the absence of measurable translational diffusion and perhaps even rotational diffusion, it would not seem to account for a net alignment of chromophores with the microvillar axes.

Laughlin et al. (1975) and Snyder and Laughlin (1975) have proposed that orientation of rhodopsin in microvillar membranes might arise from thermodynamic constraints in turning an elongate rhodopsin molecule within the curved surface of a microvillus. They postulate that an elongate protein with polar and nonpolar regions on its exterior might float in the membrane with its long axis roughly parallel to the microvillus, but that rotating it 90° about an axis normal to the surface of the membrane would cause its ends to lift out of the lipid phase and might therefore be accompanied by a significant energy barrier. Vertebrate rhodopsin in digitonin micelles is asymmetric, as it orients to shear (Wright et al., 1972, 1973). The radius of crayfish microvilli is about 350 Å (Eguchi, 1965), and minimum estimates of the length of vertebrate rhodopsin of 75 Å (Wu and Stryer, 1972) and 90 Å (Yeager, 1976) have been reported. In the latter study, evidence was also obtained that the long axis lies at right angles to the membrane, which does not support Snyder and Laughlin's model. Moreover, a 75-Å molecule rotated 90° on the surface of a cylinder 350 Å in radius has its ends lifted out of the membrane by only 2 Å. Finally, although this model speaks to the presence of axial orientation of pigment molecules, it does not predict an absence of translational diffusion.

Still another kind of mechanism that might be invoked to account both for molecular orientation and absence of measurable diffusion is attachment of the rhodopsin molecules to a relatively fixed matrix. One thinks in this context of spectrin, the membrane-associated protein of red blood cells (Marchesi and

Steers, 1968; Marchesi et al., 1976). Clearly, much more work will have to be done before the molecular architecture of these membranes is understood.

Choice of Angular Distribution Functions

Model I supposes that tilt of the absorption vector into the membrane is the same for every molecule. Model II assumes that tilt angles are uniformly distributed through all allowed angles. These two assumptions bracket a range of additional possibilities including, for example, a Boltzmann distribution over a limited range of θ. That the experimental results on photodichroism are reasonably compatible with either model shows that the specific choice of angular distribution function is not critical.

The fit of results to model I is perhaps slightly superior. If tilt angle is constant (fixed θ), the presence of photodichroism demonstrates that the transition moments must be distributed through a range of values of ϕ. Considerations of symmetry suggest that these values occur to both sides of the microvillar axis, and a Boltzmann distribution is a physically plausible supposition. Further work will be required to see whether there is any basis in experiment for favoring one of several possible mathematical models.

Change in Orientation on Isomerization

The transition moment reorients several degrees as rhodopsin is converted to metarhodopsin. The result is that the absorption vector associated with metarhodopsin is either tilted more out of the plane of the membrane, or has a reduced alignment with the microvillar axes, or both. A change of the same magnitude has also been seen in lobster (*Homarus*) (Bruno et al., 1977). Acid metarhodopsin of cephalopod mollusks reorients in the same sense, but the change (~15°) is several times larger (Taüber, 1975; Schlecht and Taüber, 1975). In frog (*Rana*) outer segments metarhodopsin I is reported to have approximately the same orientation as rhodopsin (Tokunaga et al., 1976), but more recent measurements from the same laboratory indicate that metarhodopsin I is tilted about 3° further out of the plane of the disk membrane than rhodopsin (F. Tokunaga, personal communication). Results from three phyla are thus qualitatively similar.

The hypsochromic shift in λ_{max} of crayfish rhodopsin to metarhodopsin is about 20 nm in both formaldehyde and glutaraldehyde. Moreover, the half-bandwidth of both rhodopsin and metarhodopsin is 4,550 ± 80 cm^{-1} in either formaldehyde or glutaraldehyde (Goldsmith, 1977). To a first approximation, therefore, the isomerized chromophore finds its appropriate, "metarhodopsin" relationship with the surface of the opsin in the presence of either aldehyde. A closer look, however, indicates that there are detectable differences. The reorientation of the transition moment, although small, is 3.5 times larger in formaldehyde than glutaraldehyde, regardless of which model or which parameters are used in the calculation (Table I). The reorientation of the transition moment therefore seems to involve not just isomerization of the chromophore but some concomitant shifting of the surface of the opsin as well. This shifting is constrained by a reagent that readily cross-links via bridges of variable length (Richards and Knowles, 1968).

The apparently greater molar extinction of metarhodopsin in formaldehyde- as opposed to glutaraldehyde-treated rhabdoms can be interpreted as indicating (with equal bandwidths) that the oscillator strength of metarhodopsin is reduced ~10% by glutaraldehyde. On the other hand, the same experimental result could have been caused by a small loss of metarhodopsin through photobleaching. Although the experiment was designed to minimize this possibility, a loss of metarhodopsin would be indistinguishable (in Eq. [23] and [24]) from a real decrease in the relative extinction coefficient (N/M), but would not affect conclusions about the orientation parameters. The possibility of a few percent loss of pigment cannot therefore be excluded as an alternative explanation for the lower value of N/M, but it does not account for the smaller reorientation of transition moment that is seen in glutaraldehyde.

Implications for Polarization Sensitivity

The orientation parameters estimated from the measurements of photodichroism can be used to predict the linear dichroism that should be observed in rhabdoms from dark-adapted eyes. For example, $\phi_d = 40°–50°$, $\theta_d = 40°$ (model II) corresponds to a dichroic ratio $R_0 = 5–7$ (Fig. 5 B). This is about twice the value measured on the isolated rhabdom by microspectrophotometry (Goldsmith, 1975). It is in good agreement with an average ratio of polarization sensitivity of 6.2 measured in crayfish retinular cells by Shaw (1969), although it is lower by a factor of two than the largest such values (Shaw, 1969; Waterman and Fernandez, 1970). In view of the technical differences in making these two kinds of measurement, the results of studies of photodichroism and electrophysiological studies of polarization sensitivity are in reasonable harmony. The situation would be more satisfactory, however, if we could account for the consistently lower values of dichroic ratio measured directly by microspectrophotometry. A further analysis of this problem, too lengthy for inclusion in this Discussion, will be presented elsewhere.

Several factors conceivably affecting dichroic ratio can be briefly mentioned here. (*a*) Depolarization by scatter is not a significant source of trouble (Fig. 14). (*b*) Depolarization caused by departure from collimation (the effect of numerical aperture of the condensor [Hárosi and Malerba, 1975]) degrades our dichroic ratios by only a few percent. (*c*) Departure of the microvilli from cylindrical cross-sections, to the extent it occurs, appears to be random (Eguchi, 1965). (*d*) Some relaxation of the molecules from their orientation in vivo when the rhabdoms are separated from their retinular cells is a possibility (Goldsmith, 1975), but there is no clear evidence pro or con. (*e*) Some rotational misalignment of the rhabdoms around their long axes is inevitable, but by measuring dichroic ratio in two contiguous bands of microvilli it is possible to recognize and correct for this problem (Goldsmith, 1975). (*f*) Rotational misalignment of the rhabdom about the axis of propagation of the measuring beam will produce a more serious degradation of dichroic ratio. Although such misalignment should be readily seen, its counterpart at the level of microvillar orientation is not observable in the light microscope. For example, undulating microvilli will have significantly less dichroism than straight cylinders. The relative effects of such disorganization on dichroism and photodichroism are currently being explored.

Packing Density of Photopigment

When cut in cross-section, the microvilli are seen to occupy a hexagonal lattice, and the average diameter of the microvilli is 7×10^{-2} μm (Eguchi, 1965). In making absorbance measurements on isolated rhabdoms the average path length is found to be ~25 μm. The number of microvilli traversed by the measuring beam, η, is therefore $25/(7 \times 10^{-2})$ (cos30°) = 412.

The number of molecules per unit area of membrane, n_0, can be computed from Eq. (6) (see also Eq. [18], [19], and [20]).

$$n_0 = \frac{2.3D_{0\parallel}}{\eta R_f ML(\phi, \theta)},$$

or from Eq. 7,

$$n_0 = \frac{2.3D_0^{\perp} \cdot 2}{\eta M[R_f W(\phi, \theta) + H(\phi, \theta)]}.$$

In performing the calculations, values of $\eta D_{0\parallel}$ and $\eta D_0^{\perp}$ are obtained from measurements of absorbance, and values of the normalized absorption coefficients $L(\phi, \theta)$, $W(\phi, \theta)$, and $H(\phi, \theta)$—which describe how absorbance is partitioned among α_l, α_w, and α_h—are obtained from Eq [18], [19], and [20], by using estimates of ϕ_d, θ_f, and θ_d from experiments on photodichroism. $M = 3\alpha_0$ where α_0, the Beers law molecular absorption coefficient, is assumed to be 1.56×10^{-16} cm^2, corresponding to a molar absorption coefficient (ϵ) of 40,600 liter cm^{-1} mol^{-1}. This figure, measured for vertebrate rhodopsin (Wald and Brown, 1955), is a reasonable estimate for crayfish rhodopsin, if one judges from the hydroxylamine difference spectrum published by Wald (1967).

In principle, using either Eq. 6 or Eq. 7 to calculate η_0 should give the same result. In practice, Eq. (7) yields values almost two times higher. This is because the dichroic ratio that is measured in dark-adapted rhabdoms is smaller than that calculated from Eq. (8) (by using values of ϕ_d, θ_f, and θ_d referred to above). This discrepancy was mentioned in the preceding section. On the other hand, choices of R_f and of model I or model II are relatively less important. Calculated values of η_0 are summarized in Table II and are in the range 1–2 $\times 10^{12}$ molecules cm^{-2}.

At a density of 1–2 $\times 10^{12}$ molecules cm^{-2} and on the assumption of a hexagonal lattice, the mean distance between centers of molecules is 76–107 Å.

TABLE II

CALCULATED DENSITIES OF RHODOPSIN MOLECULES PER UNIT AREA OF MICROVILLAR MEMBRANE

	R_f	n_0 (model I)	n_0 (model II)
		molecules cm^{-2}	*molecules cm*$^{-2}$
Eq. (6) ($e_{\parallel}$)	1.56	$1.01 \pm 0.34 \times 10^{12}$	$1.03 \pm 0.35 \times 10^{12}$
	1.26	$1.25 \pm 0.42 \times 10^{12}$	$1.28 \pm 0.43 \times 10^{12}$
Eq. (7) ($e_{\perp}$)	1.56	$1.85 \pm 0.87 \times 10^{12}$	$1.79 \pm 0.84 \times 10^{12}$
	1.26	$2.15 \pm 1.01 \times 10^{12}$	$2.06 \pm 0.97 \times 10^{12}$

Calculations based on Eq. (6) and (7), as described in the text. $\eta D_{0\parallel} = 0.091 \pm 0.0300$ SD; average R_0 (measured; corrected for self-screening; uncorrected for possible rotational misalignment) = 2.81 ± 0.942 SD ($\eta D_{0\perp} = \eta D_0/R_0$); $\phi_d = 50°$; $\theta_f = 20°$ (model I); $\theta_d = 40°$ (model II).

There are two recent freeze-fracture studies of crayfish microvilli in which 80–90-Å diameter particles have been observed at a similar density on the protoplasmic leaflet of the cleaved membranes. Fernandez and Nickel (1976) report that in examples showing densest packing, the center-to-center distance is 85 Å, and Eguchi and Waterman (1976) find average interparticle distances of 110 ± 10 Å. (The latter authors' evidence for turnover of particles with light adaptation further suggests that the freeze-fracture images reflect the presence of rhodopsin as well as indicating a possible reason why their average values of particle density are about 20% higher than those of Fernandez and Nickel.) As X-ray diffraction of the disk membranes of rod outer segments indicates about 70 Å between nearest rhodopsin neighbors (Blasie et al., 1969), the density of packing of visual pigment in arthropod and vertebrate photoreceptor membranes appears similar.

Values of η_0 can be converted into concentrations of pigment in the total volume of the rhabdom by the following argument. Let d be the diameter of a microvillus ($d = 7 \times 10^{-6}$ cm). The surface area of a 1-cm length of microvillus is therefore πd cm^2, and the number of microvilli in 1 cm^3 of rhabdom is $1/d \times 1/d \cos 30°$. The total membrane surface in 1 cm^3 of rhabdom is therefore $\pi/d \cos 30° = 5.18 \times 10^5$ cm^2. 1 cm^3 of rhabdom thus contains 5.18×10^5 cm$^2 \times \eta_0$ molecules. For $\eta_0 = 1\text{–}2 \times 10^{12}$, the concentration is about 0.9–1.7 mM. These estimates can be compared with values of 3.1–3.8 mM (Hárosi, 1975; Liebman, 1975) calculated for various amphibian outer segments.

Other Photoreceptors Have Oriented Pigment Molecules

The arthropod rhabdom is not the only place where photoreceptor molecules are oriented and where the system seems designed for differential response to linearly polarized light. Haupt (1972, 1973) has described the photocontrol of chloroplast orientation in the filamentous green alga *Mougeotia*. Although the pigment that mediates this response is phytochrome, the system shares several features with the crayfish rhabdom. (*a*) The pigment molecules are located in the cortical cytoplasm, either in the plasma membrane or attached to its inner surface. (*b*) The transition moments are not randomly disposed in the membrane, but have a fixed, in this case helical, pattern around the surface of the cylindrical cell. (*c*) Photoconversion of the red-absorbing form (P_{660}) to the far red-absorbing form (P_{730}) is accompanied by a significant reorientation of the absorption vector. In the P_{660} form the absorption vector lies in the tangent plane of the cylindrical cell, whereas in the P_{730} form it is tipped more nearly normal to the plasma membrane, becoming radially oriented with respect to the cylindrical cell. These conclusions, based on elegant experiments in which the cells were stimulated with microbeams of plane-polarized light, indicate a relatively rigid anchoring of the pigment molecules in a matrix either associated with or identical to the plasmalemma.

APPENDIX

Dichroism of Microvilli

Consider a cylindrical microvillus irradiated normal to its axis with collimated light, polarized either parallel, $e_\parallel$, or perpendicular, $e_\perp$, to the microvillar axis (Fig. 1). Each

molecule of pigment lies near the surface of the cylinder with its transition moment making an angle ϕ, measured in the tangent plane, with a generator of the cylinder; and an angle θ, also measured from the generator, but in the plane defined by the long axis of the cylinder and a radius of the cylinder. ϕ is thus the angle, measured in the tangent plane, between the chromophore's axis and the microvillar axis; and θ is the tilt of the chromophore's axis into the membrane.

At an arbitrary point on the circumference of the cylinder, located at an azimuthal angle ψ from a reference radius (see Fig. 1 C), the transition moments of all molecules can be resolved into three mutually perpendicular absorption vectors: α_l, parallel to the longitudinal axis of the cylinder; α_w, perpendicular to α_l and lying in the tangent plane; and α_h, lying along a radius of the cylinder.

The absorbance measured with polarized light is found by summing absorbance through all angles of ψ from 0 to 2π and averaging over 2π. For $e_\parallel$, absorbance is independent of ψ and is simply proportional to α_l. For $e_\perp$, however, absorbance is proportional to

$$\frac{\alpha_w \int_0^{2\pi} \cos^2\psi \, d\psi + \alpha_h \int_0^{2\pi} \sin^2\psi \, d\psi}{\int_0^{2\pi} d\psi} = \frac{1}{2}(\alpha_w + \alpha_h).$$

The intrinsic dichroic ratio of the cylinder, R_0', is thus given by

$$R_0' = \frac{\alpha_l}{\frac{1}{2}(\alpha_w + \alpha_h)}. \tag{1}$$

The total dichroism, R_0, is obtained after taking form dichroism into account (Snyder and Laughlin, 1975).

$$R_0 = \frac{D_{0\parallel}}{D_{0\perp}} = \frac{2R_f\alpha_l}{\alpha_h + R_f\alpha_w}, \tag{2}$$

where $R_f = \frac{n_m^4}{n_c^4}$, and n_m and n_c are refractive indices of the membrane and cytoplasm, respectively.

We shall now consider how the absorbance coefficients, α, depend upon the angular orientation of the chromophores. For each molecule (Fig. 15)

$$\alpha_l^0 = M \cos^2\phi \cos^2\theta, \tag{3}$$

$$\alpha_w^0 = M \sin^2\phi \cos^2\theta, \tag{4}$$

$$\alpha_h^0 = M \sin^2\theta, \tag{5}$$

where M is the molecular absorbance coefficient for a molecule aligned with its transition moment parallel to the e-vector of the irradiating source. For a completely random distribution of molecules, all values of θ and ϕ would be equally populated. Measured values of microvillar dichroism, however, are too high to be consistent with random orientation (Goldsmith, 1975) and imply some degree of orientation with the microvillar axes. The simplest assumption for oriented chromophores is that they are rigidly locked in the membrane at fixed angles θ_f and ϕ_f. This hypothesis, however, is not consistent with the experimental observation of photoinduced dichroism.

Building on Liebman's (1962) analysis of dichroism in rods, we have explored two models. Model I assumes that the chromophores are tilted into the membrane at some fixed angle θ_f, but that they are free to occupy all angles ϕ between limiting values $\pm\phi_d$.

Small values of ϕ_d and θ_f therefore mean relatively strong orientation with the microvillar axis. $\phi_d = \pm 90°$ corresponds to random orientation of absorption vectors in the tangent plane. Model II is similar, except that rather than the tilt angles being fixed, they are distributed between $\theta = 0$ and some limiting value $\theta = \theta_d$ ($<90°$). This is the model Liebman likened to match sticks rattling in a closed box that is too shallow to permit their tumbling end-over-end. The specific distribution functions in the range $-\phi_d < \phi < \phi_d$ and $0 < \theta < \theta_d$ must also be postulated; if we assume that all angles within these ranges are equally occupied, the absorbance of the microvillus measured with $e_{\parallel}$ is then

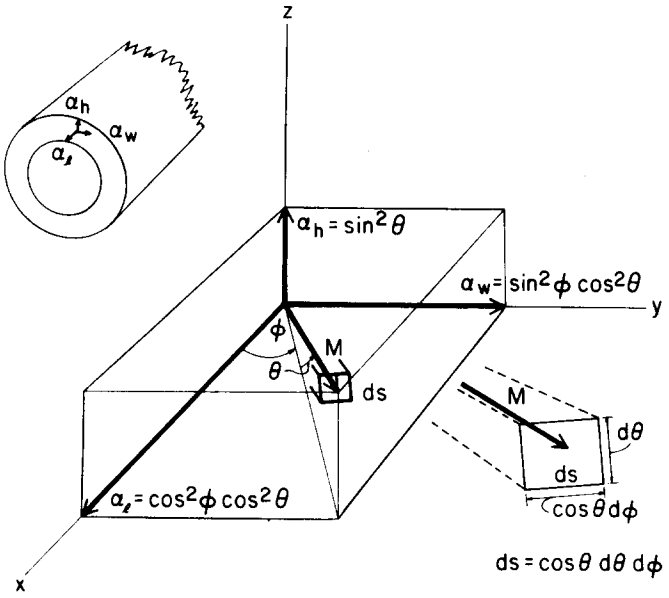

FIGURE 15. Small slab of microvillar membrane containing a chromphore with unit absorbance M, and indicating how the coefficients α_l, α_w, and α_h are related to the angles ϕ and θ. ds is an increment of solid angle (*inset*).

$$D_{0\parallel} = \frac{\frac{MR_f}{2.3}\iint n\cos^2\phi\cos^2\theta\, ds}{\iint ds}, \tag{6}$$

and absorbance of the microvillus measured with $e_{\perp}$ is

$$D_{0\perp} = \frac{\frac{M}{(2)(2.3)}\iint n\sin^2\theta\, ds + \frac{MR_f}{(2)(2.3)}\iint n\sin^2\phi\cos^2\theta\, ds}{\iint ds}, \tag{7}$$

where n is the number of molecules per unit area of membrane, and $ds = \cos\theta\, d\theta\, d\phi$, an increment of solid angle (Fig. 15). Eq. (6) and (7) are complete forms of the numerator and denominator of Eq. (2), respectively, before common terms have been canceled. The factor 2.3 enters Eq. (6) and (7) because D (absorbance) is defined in terms of base 10 logarithms, whereas the molecular absorption coefficients M and α are defined in terms of base e. Therefore, for a sheet of perfectly aligned molecules (no form dichroism), $D_{0\parallel} = Mn/2.3$. In the dark-adapted state, we assume that all allowed angles are equally

populated with absorption vectors, and n is a constant, n_0. The term R_f appears in Eq. (2) as a result of integrating through the cylindrical geometry of the microvillus (see Snyder and Laughlin, 1965, for more complete details).

The dichroic ratio of a microvillus, R_0, is obtained by dividing Eq. (6) by Eq. (7). For model I, $\theta = \theta_f$, a constant, and the integration is only performed over ϕ, from $\phi = -\phi_d$ to $\phi = \phi_d$. Thus, after multiplying numerators and denominators by $\frac{2.3}{M} \iint ds = \frac{2.3}{M} 2\phi_d \cos\theta_f$,

$$R_0 = \frac{R_f \cos^2\theta_f \int_{-\phi_d}^{\phi_d} \cos^2\phi \, d\phi}{\frac{R_f}{2} \cos^2\theta_f \int_{-\phi_d}^{\phi_d} \sin^2\phi \, d\phi + \frac{\sin^2\theta_f}{2} \int_{-\phi_d}^{\phi_d} d\phi}. \tag{8a}$$

For model II it is necessary to integrate over both ϕ and θ. After multiplying numerator and denominator by $\frac{2.3}{M} \iint ds = \frac{2.3}{M} 2\phi_d \sin\theta_d$,

$$R_0 = \frac{R_f \int_{-\phi_d}^{\phi_d} \cos^2\phi \, d\phi \int_0^{\theta_d} \cos^3\theta \, d\theta}{\frac{R_f}{2} \int_{-\phi_d}^{\phi_d} \sin^2\phi \, d\phi \int_0^{\theta_d} \cos^3\theta \, d\theta + \frac{1}{2} \int_{-\phi_d}^{\phi_d} d\phi \int_0^{\theta_d} \sin^2\theta \cos\theta \, d\theta}. \tag{8b}$$

For $\phi_d = 90°$ and θ_d (or θ_f) = 0, the molecules are randomly oriented in the tangent planes of the microvilli, the case described by Moody and Parriss (1961).

Calculated values of dichroic ratio as a function of ϕ_d for several values of θ_d for model II are shown in Fig. 5 with the curves labeled R_0. The limiting cases of tilt angle (θ_d = 0; θ_d = 90°) are shown in Fig. 5 A. One can calculate that for frog rods θ_d = 36.8°–41.3°, corresponding to dichroic ratios of 4–5 (Liebman, 1962; Hárosi and MacNichol, 1974*a*, *b*; Hárosi, 1975), and a form dichroism of 1.36 (Liebman et al., 1974). The curve in Fig. 5 B labeled θ_d = 40° therefore shows the approximate microvillar dichroism if the pigment molecules in rod disk membranes and crayfish microvillar membranes have the same distribution of tilt angles. Similar curves are obtained for model I, with θ_f about half as large as θ_d.

Photoinduced Dichroism of Microvilli

If a bleaching light polarized parallel to the microvillar axis ($e_\parallel$) is imposed on the system, the number of bleached molecules per unit area, n_b, at θ and ϕ is proportional to their initial absorbance. Thus, from Eq. (6),

$$n_b = k_\parallel n_0 2R_f \cos^2\phi \cos^2\theta,$$

where $k_\parallel$ is a proportionality constant. The remaining pigment per unit area is obtained from $n_p = n_0 - n_b$. Therefore

$$n_p = n_0(1 - 2R_f k_\parallel \cos^2\phi \cos^2\theta). \tag{9}$$

The coefficient $k_\parallel$ expresses the extent of the bleach and is determined by considering bleaching at the most vulnerable angles. As photons ($e_\parallel$) are delivered, n_p first reaches zero at $\phi = 0$ and $\theta = 0$ (model II), which is the orientation of transition moment giving optimal absorption. Under these conditions Eq. (9) yields

$$k_{\parallel max} = 1/(2R_f \cos^2\theta_f) \tag{10a}$$

for model I, and

$$k_{\parallel \max} = 1/(2R_f) \tag{10b}$$

for model II.

In what follows we shall be concerned only with fractional bleaches in which $k_\parallel \leq k_{\parallel \max}$, so that angles other than the optimal angle are never completely depopulated.

Absorbance measured with $e_\parallel$ ($D_\parallel$) after a fractional bleach with $e_\parallel$ is obtained by substituting n_p (Eq. [9]) for n in Eq. (6). Likewise, absorbance measured with $e_\perp$ ($D_\perp$) is found by substituting n_p (Eq. [9]) for n in Eq. (7). The new dichroic ratio, $R_\parallel = D_\parallel/D_\perp$, is then given by Eq. (11*a*) (integrating over ϕ only; model I) or Eq. (11*b*) (integrating over both ϕ and θ; model II). In evaluating Eq. (11*a*) and (11*b*), $0 < k < k_{\parallel \max}$, as described in the preceding paragraph.

$$R_\parallel = \frac{R_f \cos^2\theta_f \int_{-\phi_d}^{\phi_d} \cos^2\phi \, d\phi - R_f k_\parallel \cos^4\theta_f \int_{-\phi_d}^{\phi_d} \cos^4\phi \, d\phi}{\left\{ \begin{array}{l} \frac{R_f}{2} \cos^2\theta_f \int_{-\phi_d}^{\phi_d} \sin^2\phi \, d\phi + \phi_d \sin^2\theta_f - \frac{R_f}{2} k_\parallel \cos^4\theta_f \int_{-\phi_d}^{\phi_d} \cos^2\phi \sin^2\phi \, d\phi \\ \qquad - \frac{k_\parallel}{2} \sin^2\theta_f \cos^2\theta_f \int_{-\phi_d}^{\phi_d} \cos^2\phi \, d\phi \end{array} \right\}}. \tag{11a}$$

For model II,

$$R_\parallel = \frac{R_f \int_{-\phi_d}^{\phi_d} \cos^2\phi \, d\phi \int_0^{\theta_d} \cos^3\theta \, d\theta - 2R_f k_\parallel \int_{-\phi_d}^{\phi_d} \cos^4\phi \, d\phi \int_0^{\theta_d} \cos^5\theta \, d\theta}{\left\{ \begin{array}{l} \frac{R_f}{2} \int_{-\phi_d}^{\phi_d} \sin^2\phi \, d\phi \int_0^{\theta_d} \cos^3\theta \, d\theta + \phi_d \int_0^{\theta_d} \sin^2\theta \cos\theta \, d\theta \\ \qquad - R_f k_\parallel \int_{-\phi_d}^{\phi_d} \cos^2\phi \, d\phi \int_0^{\theta_d} \sin^2\theta \cos^3\theta \, d\theta \\ \qquad - R_f^2 k_\parallel \int_{-\phi_d}^{\phi_d} \sin^2\phi \cos^2\phi \, d\phi \int_0^{\theta_d} \cos^5\theta \, d\theta \end{array} \right\}} \tag{11b}$$

The dichroic ratio after a fractional bleach with $e_\perp$ is found by an analogous argument. After a bleach with $e_\perp$, the fraction of pigment remaining depends on ϕ and θ as

$$n_p = n_o[1 - k_\perp(\sin^2\theta + R_f \sin^2\phi \cos^2\theta)]. \tag{12}$$

With the bleaching light polarized $e_\perp$, the molecules that are optimally oriented for absorption will be found at $\pm\phi_d$ and at θ_d or θ_f. As a consequence, the most vulnerable chromophores in the microvillus depend on the relative magnitudes of α_h and $R_f\alpha_w$. With model I, the contribution of chromophores oriented at $\pm\phi_d$ to α_w is proportional to $R_f \cos^2\theta_f \sin^2\phi_d$. On the other hand, all molecules contribute equally to α_h. Chromophores in any angle ϕ in the range $-\phi_d < \phi < \phi_d$ therefore contribute an absorption of $\alpha_h/2\phi_d$ to α_h; and specifically, those chromophores at $\pm\phi_d$ contribute twice this, an amount proportional to $\sin^2\theta_f/\phi_d$ (see Eq. [20 *a*]). Therefore if $\frac{\sin^2\theta_f}{\phi_d} R_f \cos^2\theta_f \sin^2\phi_d$

$$k_{\perp \max} = \phi_d/\sin^2\theta_f \tag{13a}$$

When the second term in the inequality is larger, however,

$$k_{\perp \max} = 1/(R_f \cos^2\theta_f \sin^2\phi_d). \tag{13b}$$

Similarly, with model II, for $\sin^2\theta_d > R_f \sin^2\phi_d$

$$k_{\perp max} = 1/\sin^2\theta_d, \tag{13c}$$

and for $\sin^2\theta_d < R_f \sin^2\phi_d$,

$$k_{\perp max} = 1/(R_f \sin^2\phi_d). \tag{13d}$$

As with $e_\parallel$, we treat only partial bleaches that do not totally depopulate any but the optimal angle.

The absorbance $D_\parallel$ after a fractional bleach with $e_\perp$ is found by substituting n_p (Eq. [12]) for n in Eq. (6). Similarly, $D_\perp$ is obtained by substituting n_p (Eq. [12]) for n in Eq. (7). The new dichroic ratio, $R_\perp = D_\parallel/D_\perp$ is then given by Eq. 14*a* (model I) or 14*b* (model II).

Model I

$$R_\perp = \frac{\left\{\begin{array}{c} R_f \cos^2\theta_f \displaystyle\int_{-\phi_d}^{\phi_d} \cos^2\phi\, d\phi - R_f k_\perp \cos^2\theta_f \sin^2\theta_f \int_{-\phi_d}^{\phi_d} \cos^2\phi\, d\phi \\ - R_f^2 k_\perp \cos^4\theta_f \displaystyle\int_{-\phi_d}^{\phi_d} \cos^2\phi \sin^2\phi\, d\phi \end{array}\right\}}{\left\{\begin{array}{c} \frac{R_f}{2} \cos^2\theta_f \displaystyle\int_{-\phi_d}^{\phi_d} \sin^2\phi\, d\phi + \phi_d \sin^2\theta_f - k_\perp \phi_d \sin^4\theta_f \\ - R_f k_\perp \sin^2\theta_f \cos^2\theta_f \displaystyle\int_{-\phi_d}^{\phi_d} \sin^2\phi\, d\phi - \frac{k_\perp}{2} R_f^2 \cos^4\theta_f \int_{-\phi_d}^{\phi_d} \sin^4\phi\, d\phi \end{array}\right\}}. \tag{14a}$$

Model II

$$R_\perp = \frac{\left\{\begin{array}{c} R_f\left[\displaystyle\int_{-\phi_d}^{\phi_d} \cos^2\phi\, d\phi \int_0^{\theta_d} \cos^3\theta\, d\theta - k_\perp \int_{-\phi_d}^{\phi_d} \cos^2\phi\, d\phi \int_0^{\theta_d} \cos^3\theta \sin^2\theta\, d\theta\right. \\ \left. - R_f k_\perp \displaystyle\int_{-\phi_d}^{\phi_d} \sin^2\phi \cos^2\phi\, d\phi \int_0^{\theta_d} \cos^5\theta\, d\theta\right] \end{array}\right\}}{\left\{\begin{array}{c} \frac{R_f}{2} \displaystyle\int_{-\phi_d}^{\phi_d} \sin^2\phi\, d\phi \int_0^{\theta_d} \cos^3\theta\, d\theta + \phi_d \int_0^{\theta_d} \sin^2\theta \cos\theta\, d\theta \\ - k_\perp \phi_d \displaystyle\int_0^{\theta_d} \sin^4\theta \cos\theta\, d\theta - R_f k_\perp \int_{-\phi_d}^{\phi_d} \sin^2\phi\, d\phi \int_0^{\theta_d} \cos^3\theta \sin^2\theta\, d\theta \\ - \frac{R_f^2}{2} k_\perp \displaystyle\int_{-\phi_d}^{\phi_d} \sin^4\phi\, d\phi \int_0^{\theta_d} \cos^5\theta\, d\theta \end{array}\right\}}. \tag{14b}$$

As before, in evaluating Eq. (14*a*) or (14*b*) we observe the condition $0 < k < k_{\perp max}$. The curves in Fig. 5, denoted $R_\parallel$ and $R_\perp$, show computed results for Eq. 11*b* and 14*b* for $k = k_{max}$.

For comparison with experimental data, we define photoinduced dichroism after bleaching with $e_\parallel$ as the dichroic ratio before the actinic exposure divided by the dichroic ratio after exposure, $R_0/R_\parallel$. In the case of bleaches with $e_\perp$, it is the reciprocal, $R_\perp/R_0$. Photoinduced dichroism, a ratio of ratios, is therefore a positive number greater than unity and is calculated from Eq. (8), (11), and (14) for various values of $k_\parallel/k_{\parallel max}$, and $k_\perp/k_{\perp max}$. Although the coefficients $k_\parallel$ and $k_\perp$ are not directly measurable, the fraction of pigment bleached in the polarization axis of the actinic beam is and can be computed from the numerators of Eq. (8), (11), and (14) for $e_\parallel$, and the denominators for $e_\perp$. For $e_\parallel$,

the fraction bleached is $(D_{0\parallel} - D_{\parallel})/D_{0\parallel}$; and for $e_\perp$, the fraction bleached is $(D_{0\perp} - D_\perp)/D_{0\perp}$. Photoinduced dichroism and fraction bleached are the functions plotted in Figs. 9–11.

As pointed out above, Eq. (11) and (14) do not describe dichroic ratio over the complete range of bleaching. They are valid only when the irradiating exposure is small enough that none other than the most vulnerable angle is completely bleached. This is why the theoretical curves in Fig. 9 do not cover all values of "fraction bleached"; the curves terminate near points set by the definitions of $k_{\parallel max}$ and $k_{\perp max}$. This limitation, however, is of no practical consequence in comparing theory with experimental data. The reason is that as fraction bleached approaches 1.0 and the photodichroism increases steeply, the accuracy of measurement deteriorates precipitously, because one of the absorbance values sinks into the noise level.

Changes in Molecular Orientation on Isomerization; Relative Molar Absorbance of Pigment and Photoproduct

In solution, the difference spectrum associated with the isomerization of rhodopsin to metarhodopsin reflects the fact that the absorbance spectra of these two forms are not identical. In the rhabdom, the difference spectrum also depends on the plane of polarization of the measuring light, indicating that isomerization is accompanied by a change in molecular orientation (see Figs. 12, 13). Heretofore we have written absorbance coefficients for the pigment, α_l, α_w, and α_h (Eq. [3–5]; Fig. 15). Now it becomes necessary to distinguish more carefully between rhodopsin and its photoproduct by defining three corresponding coefficients, β_l, β_w, and β_h for the metarhodopsin.

Reiterating the argument that underlies Eq. (6) and (7), the normalized absorbance coefficients for rhodopsin can be written

$$L(\phi, \theta) = \alpha_l/M = \frac{\iint \cos^2\phi \cos^2\theta \, ds}{\iint ds}, \tag{15a}$$

$$W(\phi, \theta) = \alpha_w/M = \frac{\iint \sin^2\phi \cos^2\theta \, ds}{\iint ds}, \tag{16a}$$

$$H(\phi, \theta) = \alpha_h/M = \frac{\iint \sin^2\theta \, ds}{\iint ds}, \tag{17a}$$

where M is the molecular absorbance coefficient for rhodopsin perfectly oriented parallel to the plane of polarization of the measuring light. Similar functions can also be written for metarhodopsin,

$$L'(\phi, \theta) = \beta_l/N, \tag{15b}$$

$$W'(\phi, \theta) = \beta_w/N, \tag{16b}$$

$$H'(\phi, \theta) = \beta_h/N,$$

where N is the molecular absorbance coefficient for perfectly oriented metarhodopsin. Specifically, integrating Eq. (6) and (7) in the case of model I,

$$L(\phi_d, \theta_f) = \frac{\cos^2\theta_f}{2\phi_d}\int_{-\phi_d}^{\phi_d}\cos^2\phi\, d\phi = \cos^2\theta_f\left[\frac{1}{2} + \frac{\sin 2\phi_d}{4\phi_d}\right], \tag{18a}$$

$$W(\phi_d, \theta_f) = \frac{\cos^2\theta_f}{2\phi_d}\int_{-\phi_d}^{\phi_d}\sin^2\phi\, d\phi = \cos^2\theta_f\left[\frac{1}{2} - \frac{\sin 2\phi_d}{4\phi_d}\right], \tag{19}$$

$$H(\phi_d, \theta_f) = \sin^2\theta_f. \tag{20a}$$

The corresponding normalized absorbance coefficients for metarhodopsin differ by the substitution of θ_f' for θ_f (if tilt angle changes on isomerization), and ϕ_d' for ϕ_d (if the fan of axial orientations changes).

For model II,

$$L(\phi_d, \theta_f) = \frac{\int_{-\phi_d}^{\phi_d}\cos^2\phi\, d\phi \int_0^{\theta_d}\cos^3\theta\, d\theta}{2\phi_d \sin\theta_d} = \left[\frac{1}{2} + \frac{\sin 2\phi_d}{4\phi_d}\right]\left[\frac{\cos^2\theta_d + 2}{3}\right], \tag{18b}$$

$$W(\phi_d, \theta_f) = \frac{\int_{-\phi_d}^{\phi_d}\sin^2\phi\, d\phi \int_0^{\theta_d}\cos^3\theta\, d\theta}{2\phi_d \sin\theta_d} = \left[\frac{1}{2} - \frac{\sin 2\phi_d}{4\phi_d}\right]\left[\frac{\cos^2\theta_d + 2}{3}\right], \tag{19b}$$

$$H(\phi_d, \theta_d) = \frac{\int_0^{\theta_d}\sin^2\theta\cos\theta\, d\theta}{\sin\theta_d} = \frac{\sin^2\theta_d}{3}. \tag{20b}$$

$L'(\phi, \theta)$, $W'(\phi, \theta)$, and $H'(\phi, \theta)$ are obtained by substituting ϕ_d' for ϕ_d and θ_d' for θ_d. Note that $L(\phi, \theta) + W(\phi, \theta) + H(\phi, \theta) = 1$ and $L'(\phi, \theta) + W'(\phi, \theta) + H'(\phi, \theta) = 1$.

The change in absorbance on isomerization—the difference spectrum—is

$$2.3\Delta D_{\parallel}(\lambda) = R_f[b(\lambda)\,\beta_l - a(\lambda)\,\alpha_l], \tag{21a}$$

$$2.3\Delta D_{\perp}(\lambda) = \frac{R_f}{2}[b(\lambda)\,\beta_w - a(\lambda)\,\alpha_w] + \frac{1}{2}[b(\lambda)\,\beta_h - a(\lambda)\,\alpha_h], \tag{22a}$$

where ΔD is the absorbance change per unit path length and concentration,

$$a(\lambda) = \frac{\epsilon_{(\lambda)}^{rhod}}{\epsilon_{\lambda_{max}}^{rhod}} = \frac{M(\lambda)}{M_{\lambda_{max}}}, \quad \text{and} \quad b(\lambda) = \frac{\epsilon_{(\lambda)}^{meta}}{\epsilon_{\lambda_{max}}^{meta}} = \frac{N(\lambda)}{N_{\lambda_{max}}}.$$

The functions $a(\lambda)$ and $b(\lambda)$ are therefore the relative absorbance spectra of rhodopsin and metarhodopsin, and can be determined from experimentally measured difference spectra for total bleaches, as presented in Goldsmith (1977).

We can write for the absorbance changes at two selected wavelengths near the positive and negative peaks of the difference spectra

$$-\Delta D_{\parallel 575} = \frac{R_f}{2.3}[a_{575}\,\alpha_l - b_{575}\,\beta_l], \tag{21b}$$

$$\Delta D_{\parallel 475} = \frac{R_f}{2.3}[b_{475}\,\beta_l - a_{475}\,\alpha_l]. \tag{21c}$$

Let $Q_{\parallel} = \Delta D_{\parallel 475}/-\Delta D_{\parallel 575}$. $Q_{\parallel}$ is measured directly from the normalized difference spectrum (Figs. 12, 13).

Combining Eq. (21*b*), (21*c*), (15*a*), and (15*b*), and rearranging,

$$\frac{N}{M} = \frac{[1.0 - W(\phi, \theta) - H(\phi, \theta)][Q_{\parallel}a_{575} + a_{475}]}{L'(\phi, \theta)[Q_{\parallel}b_{575} + b_{475}]}. \tag{23}$$

The data measured with $e_\perp$ can be treated in a similar fashion:

$$-\Delta D_{\perp 575} = \frac{R_f}{(2.3)(2)}[a_{575}\,\alpha_w - b_{575}\,\beta_w] + \frac{1}{(2.3)(2)}[a_{575}\,\alpha_h - b_{575}\,\beta_h], \tag{22b}$$

$$\Delta D_{\perp 475} = \frac{R_f}{(2.3)(2)}[b_{475}\,\beta_w - a_{475}\,\alpha_w] + \frac{1}{(2.3)(2)}[b_{475}\,\beta_h - a_{475}\,\alpha_h]. \tag{22c}$$

Let $Q_\perp = \Delta D_{\perp 475}/-\Delta D_{\perp 575}$.

Combining Eq. (16*a*), (16*b*), (17*a*), (17*b*), (22*b*), and (22*c*) and rearranging,

$$\frac{N}{M} = \frac{[W(\phi,\theta)R_f + H(\phi,\theta)][Q_\perp a_{575} + a_{475}]}{[W'(\phi,\theta)R_f + H'(\phi,\theta)][Q_\perp b_{575} + b_{475}]}. \tag{24}$$

To restate the problem, we would like to know N/M, the relative extinction coefficient, as well as how ϕ_d' and θ_d' (or θ_f') differ from the original angles ϕ_d and θ_d (or θ_f). The answers lie in Eq. (23) and (24). As described, the coefficients $Q_\parallel$, $Q_\perp$, a_{575}, a_{475}, b_{575}, and b_{475} can be measured in experiments, as in principle can R_f. The parameters $\phi_d' = 40° - 50°$, $\theta_d' = 40°$, and $\theta_f' = 20°$ provide a reasonable fit to the data on photodichroism (Fig. 11), and can be used in Eq. (18), (19), and (20) to calculate $L'(\phi,\theta)$, $W'(\phi,\theta)$, and $H'(\phi,\theta)$.

By replacing $W(\phi,\theta)$ and $H(\phi,\theta)$ with their integrated forms (Eq. [19] and [20]), we see that the two equations, (23) and (24), involve three unknowns, (N/M), ϕ_d, and θ_d (or θ_f). This is not the impasse it might appear to be, for it is possible to obtain a reasonable estimate of the magnitude of the orientation changes that accompany isomerization by assuming, first, that all changes occur in ϕ_d and the tilt angle remains constant ($\theta_d = \theta_d'$ or $\theta_f = \theta_f'$). Eq. (23) and (24) are then solved for N/M and ϕ_d. Next, similar calculations are repeated on the assumption that only tilt angle θ_d (or θ_f) changes, while axial orientation remains constant ($\phi_d = \phi_d'$). Solution of Eq. (23) and (24) now yields θ_d (or θ_f) and another value for N/M. Representative numerical results are given in Table I and are further described in Results.

Note added in proof: The calculated areal density of rhodopsin of $1\text{-}2 \times 10^{12}$ molecules cm^{-2} is in fair agreement with a figure of 0.8×10^{12} cm^{-2} that Lisman and Bering (1977. *J. Gen. Physiol.* **70.** In press) report for *Limulus* photoreceptors, on the basis of electrophysiological measurements.

We are grateful to Dr. Gary D. Bernard for many helpful discussions.

The research of Timothy H. Goldsmith is supported by United States Public Health Service grant EY00222. Rüdiger Wehner received support from grant 3.814.72 of the Swiss National Science Foundation and from the University of Zurich, and was a Rand Fellow of the Marine Biological Laboratory, Woods Hole, Mass., during the tenure of this work.

Received for publication 3 November 1976.

REFERENCES

BENOLKEN, R. M., R. E. ANDERSON, and M. B. MAUDE. 1975. Lipid composition of *Limulus* photoreceptor membranes. *Biochim. Biophys. Acta.* **413:**234–242.

BLASIE, J. K., C. R. WORTHINGTON, and M. M. DEWEY. 1969. Molecular localization of frog receptor photopigment by electron microscopy and low-angle X-ray diffraction. *J. Mol. Biol.* **39:**407–416.

BROWN, P. K. (1972). Rhodopsin rotates in the visual receptor membrane. *Nat. New Biol.* **236:**35–38.

BRUNO, M. S., S. N. BARNES, and T. H. GOLDSMITH. 1977. The visual pigment and visual cycle of the lobster *Homarus*. *J. Comp. Physiol.* In press.

CONE, R. A. 1972. Rotational diffusion of rhodopsin in the visual receptor membrane. *Nat. New Biol.* **236**:39–43.

DAEMEN, F. J. M. 1973. Vertebrate rod outer segment membranes. *Biochim. Biophys. Acta.* **300**:255–288.

EDIDIN, M. 1974. Rotational and translational diffusion in membranes. *Annu. Rev. Biophys. Bioeng.* **3**:179–201.

EDIDIN, M., Y. ZAGYANSKY, and T. J. LARDNER. 1976. Measurement of membrane protein lateral diffusion in single cells. *Science (Wash. D.C.).* **191**:466–468.

EGUCHI, E. 1965. Rhabdom structure and receptor potentials in single crayfish retinular cells. *J. Cell. Comp. Physiol.* **66**:411–430.

EGUCHI, E., and T. H. WATERMAN. 1976. Freeze-etch and histochemical evidence for cycling in crayfish photoreceptor membranes. *Cell Tissue Res.* **169**:419–434.

ELETR, S., and A. D. KEITH. 1972. Spin-label studies of dynamics of lipid alkyl chains in biological membranes: role of unsaturated sites. *Proc. Natl. Acad. Sci. U. S. A.* **69**:1353–1357.

FERNANDEZ, H. R., and E. E. NICKEL, 1976. Ultrastructural and molecular characteristics of crayfish photoreceptor membranes. *J. Cell Biol.* **69**:721–732.

GOLDMAN, L. J., S. N. BARNES, and T. H. GOLDSMITH. 1975. Microspectrophotometry of rhodopsin and metarhodopsin in the moth *Galleria*. *J. Gen. Physiol.* **66**:383–404.

GOLDSMITH, T. H. 1972. The natural history of invertebrate pigments. *In* Handbook of Sensory Physiology. Vol. VII/1. Photochemistry of Vision. H. J. A. Dartnall, editor. Springer-Verlag, Berlin. 685–719.

GOLDSMITH, T. H. 1975. The polarization sensitivity-dichroic absorption paradox in arthropod photoreceptors. *In* Photoreceptor Optics. A. W. Snyder and R. Menzel, editors. Springer-Verlag, Berlin. 392–409.

GOLDSMITH, T. H. 1977. The spectral absorption of crayfish rhabdoms: pigment, photoproduct, and pH sensitivity. *Vision Res.* In press.

GOLDSMITH, T. H., and R. WEHNER. 1975. Photo-induced dichroism in a rhabdomeric photoreceptor: evidence for restricted rotation of pigment molecules. *Biol. Bull. (Woods Hole).* **149**:427–428.

HAGINS, W. A., and P. A. LIEBMAN. 1963. The relationship between photochemical and electrical processes in living squid photoreceptors. Abstracts of the 7th Annual Meeting of the Biophysical Society.

HAGINS, W. A., and R. E. MCGAUGHY. 1967. Molecular and thermal origins of fast photoelectric effects in the squid retina. *Science (Wash. D.C.).* **157**:813–816.

HÁROSI, F. I. 1975. Absorption spectra and linear dichroism of some amphibian photoreceptors. *J. Gen. Physiol.* **66**:357–382.

HÁROSI, F. I., and E. F. MACNICHOL, JR. 1974*a*. Visual pigments of goldfish cones: spectral properties and dichroism. *J. Gen. Physiol.* **63**:279–304.

HÁROSI, F. I., and E. F. MACNICHOL, JR. 1974*b*. Dichroic microspectrophotometer: a computer-assisted, rapid, wavelength-scanning photometer for measuring linear dichroism in single cells. *J. Opt. Soc. Am.* **64**:903–918.

HÁROSI, F. I., and F. E. MALERBA. 1975. Plane-polarized light in microspectrophotometry. *Vision Res.* **15**:379–388.

HAUPT, W. 1972. Perception of light direction in oriented displacements of cell organelles. *Acta Protozool.* **11**:179–189.

HAUPT. W. 1973. Role of light in chloroplast movement. *Bioscience.* **23**:289–296.

HAYS, D., and T. H. GOLDSMITH. 1969. Microspectrophotometry of the visual pigment of the spider crab *Libinia emarginata*. *Z. Vgl. Physiol.* **65**:218–232.

HENDERSON, R., and P. N. T. UNWIN. 1975. Three-dimensional model of purple membrane obtained by electron microscopy. *Nature (Lond.)*. **257**:28–32.

HUBBARD, R., and R. C. C. ST. GEORGE. 1958. The rhodopsin system of the squid. *J. Gen. Physiol.* **41**:501–528.

ISRAELACHVILI, J. N., R. A. SAMMUT, and A. W. SNYDER. 1976. Birefringence and dichroism of photoreceptors. *Vision Res.* **16**:47–52.

ISRAELACHVILI, J. N., and M. WILSON. 1976. Absorption characteristics of oriented photopigments in microvilli. *Biol. Cybernetics.* **21**:9–15.

LAUGHLIN, S. B., R. MENZEL, and A. W. SNYDER. 1975. Membranes, dichroism and receptor sensitivity. *In* Photoreceptor Optics. A. W. Snyder and R. Menzel, editors. Springer-Verlag, Berlin. 237–259.

LIEBMAN, P. A. 1962. *In situ* microspectrophotometric studies on the pigments of single retinal rods. *Biophys. J.* **2**:161–178.

LIEBMAN, P. A. 1975. Birefringence, dichroism and rod outer segment structure. *In* Photoreceptor Optics. A. W. Snyder and R. Menzel, editors. Springer-Verlag, Berlin. 199–214.

LIEBMAN, P. A., and G. ENTINE. 1964. Sensitive low-light-level microspectrophotometer: detection of photosensitive pigments of retinal cones. *J. Opt. Soc. Am.* **54**:1451–1459.

LIEBMAN, P. A., and G. ENTINE. 1974. Lateral diffusion of visual pigment in photoreceptor disk membranes. *Science (Wash. D. C.)*. **185**:457–459.

LIEBMAN, P. A., W. S. JAGGER, M. W. KAPLAN, and F. G. BARGOOT. 1974. Membrane structure changes in rod outer segments associated with rhodopsin bleaching. *Nature (Lond.)*. **251**:31–37.

LOEW, E. R. 1976. Light, and photoreceptor degeneration in the Norway lobster, *Nephrops norwegicus* (L). *Proc. R. Soc. Lond. Ser. Biol. Sci.* **193**:31–44.

MARCHESI, V. T., H. FURTHMAYR, and M. TOMITA. 1976. The red cell membrane. *Annu. Rev. Biochem.* **45**:667–698.

MARCHESI, V. T., and E. STEERS, JR. 1968. Selective solubilization of a protein component of the red cell membrane. *Science (Wash. D. C.)*. **159**:203–204.

MASON, W. T., R. S. JAGER, and E. W. ABRAHAMSON. 1973. Characterization of the lipid composition of squid rhabdome outer segments. *Biochim. Biophys. Acta.* **306**:67–73.

MOODY, M. F., and J. R. PARRISS. 1961. The discrimination of polarized light by *Octopus*: a behavioural and morphological study. *Z. Vgl. Physiol.* **44**:268–291.

MOTE, M. I. 1974. Polarization sensitivity: a phenomenon independent of stimulus intensity or state of adaptation in retinular cells of the crabs *Carcinus* and *Callinectes*. *J. Comp. Physiol.* **90**:389–403.

MULLER, K. J. 1973. Photoreceptors in the crayfish compound eye; electrical interactions between cells as related to polarized light sensitivity. *J. Physiol. (Lond.)*. **232**:573–595.

MURATA, N., J. H. TROUGHTON, and D. C. FORK. 1975. Relationships between the transition of the physical phase of membrane lipids and photosynthetic parameters in *Anacystis nidulans* and lettuce and spinach chloroplasts. *Plant Physiol.* **56**:508–517.

OVERATH, P., H. U. SCHAIRER, and W. STOFFEL. 1970. Correlation of in vivo and in vitro phase transitions of membrane lipids in *Escherichia coli*. *Proc. Natl. Acad. Sci. U. S. A.* **67**:606–612.

POO, M., and R. A. CONE. 1974. Lateral diffusion of rhodopsin in the photoreceptor membrane. *Nature (Lond.)*. **247**:438–441.

RICHARDS, F. M., and J. R. KNOWLES. 1968. Glutaraldehyde as a protein cross-linking reagent. *J. Mol. Biol.* **37**:231–233.

SCHLECHT, P., and U. TÄUBER. 1975. The photochemical equilibrium in rhabdomeres of

Eledone and its effect on dichroic absorption. *In* Photoreceptor Optics. A. W. Snyder and R. Menzel, editors. Springer-Verlag, Berlin. 316–335.

SHAW, S. R. 1969. Sense-cell structure and interspecies comparisons of polarized-light absorption in arthropod compound eyes. *Vis. Res.* **9:**1031–1040.

SINGER, S. J., and G. L. NICOLSON. 1972. The fluid mosaic model of the structure of cell membranes. *Science (Wash. D.C.).* **175:**720–731.

SNYDER, A. W., and S. B. LAUGHLIN. 1975. Dichroism and absorption by photoreceptors. *J. Comp. Physiol.* **100:**101–116.

STEIM, J. M., M. E. TOURTELLOTTE, J. C. REINERT, R. N. MCELHANEY, and R. I. RADER. 1969. Calorimetric evidence for the liquid-crystalline state of lipids in a biomembrane. *Proc. Natl. Acad. Sci. U. S. A.* **63:**104–109.

TAÜBER, U. 1975. Photokinetics and dichroism of visual pigments in the photoreceptors of *Eledone (Ozœna) moshata. In* Photoreceptor Optics. A. W. Snyder and R. Menzel, editors. Springer-Verlag, Berlin. 296–315.

TOKUNAGA, F., S. KAWAMURA, and T. YOSHIZAWA. 1976. Analysis by spectral difference of the orientational change of the rhodopsin chromophore during bleaching. *Vision Res.* **16:**633–641.

VAN HARREVELD, A. D. 1936. A physiological solution for fresh-water crustaceans. *Proc. Soc. Exp. Biol. Med.* **34:**428–432.

WALD, G. 1967. Visual pigments of crayfish. *Nature (Lond.).* **215:**1131–1133.

WALD, G., and P. K. BROWN. 1955. The molar extinction of rhodopsin. *J. Gen. Physiol.* **38:**623–681.

WALD, G., P. K. BROWN, and I. R. GIBBONS. 1963. The problem of visual excitation. *J. Opt. Soc. Am.* **53:**20–35.

WATERMAN, T. H., and H. R. FERNANDEZ. 1970. E-vector and wavelength discrimination by retinular cells of the crayfish *Procambarus. Z. Vgl. Physiol.* **68:**154–174.

WATERMAN, T. H., H. R. FERNANDEZ, and T. H. GOLDSMITH. 1969. Dichroism of photosensitive pigment in rhabdoms of the crayfish *Orconectes. J. Gen. Physiol.* **54:**415–432.

WEHNER, R., and T. H. GOLDSMITH. 1975. Restrictions on translational diffusion of metarhodopsin in the membranes of a rhabdomeric photoreceptor. *Biol. Bull. (Woods Hole).* **149:**450.

WRIGHT, W. E., P. K. BROWN, and G. WALD. 1972. The orientation of rhodopsin and other pigments in dry films. *J. Gen. Physiol.* **59:**201–212.

WRIGHT, W. E., P. K. BROWN, and G. WALD. 1973. Orientation of intermediates in the bleaching of shear-oriented rhodopsin. *J. Gen. Physiol.* **62:**509–522.

WU, C.-W., and L. STRYER. 1972. Proximity relationships in rhodopsin. *Proc. Natl. Acad. Sci. U. S. A.* **69:**1104–1108.

YEAGER, M. 1976. Neutron diffraction analysis of the structure of retinal photoreceptor membranes and rhodopsin. Brookhaven Symposium in Biology, Neutron Scattering for the Analyses of Biological Structures. **27:**III-3-III-35.

ZINKLER, D. 1975. Zum lipidmuster der photorezeptoren von Insekten. *Verh. Dtsch. Zool. Ges.* **67**(Bochum):28–32.